

# A subadult individual of *Styracosaurus albertensis* (Ornithischia: Ceratopsidae) with comments on ontogeny and intraspecific variation in *Styracosaurus* and *Centrosaurus*

Caleb M. Brown<sup>1,\*</sup>, Robert B. Holmes<sup>2</sup>, Philip J. Currie<sup>2</sup>

<sup>1</sup>Royal Tyrrell Museum of Palaeontology, Box 7500, Drumheller, AB, T0J 0Y0, Canada; caleb.brown@gov.ab.ca

<sup>2</sup>Department of Biological Sciences, University of Alberta, Edmonton, Alberta, T6G 2E9, Canada; holmes1@ualberta.ca; philip.currie@ualberta.ca

**Abstract:** *Styracosaurus albertensis* is an iconic centrosaurine horned dinosaur from the Campanian of Alberta, Canada, known for its large spike-like parietal processes. Although described over 100 years ago, subsequent discoveries were rare until the last few decades, during which time several new skulls, skeletons, and bonebeds were found. Here we described an immature individual, the smallest known for the species, represented by a complete skull and fragmentary skeleton. Although ~80% maximum size, it possesses a suite of characters associated with immaturity, and is regarded as a subadult. The ornamentation is characterized by a small, recurved, but fused nasal horncore; short, rounded postorbital horncores; and short, triangular, and flat parietal processes. Using this specimen, and additional skulls and bonebed material, the cranial ontogeny of *Styracosaurus* is described, and compared to *Centrosaurus*. In early ontogeny, the nasal horncores of *Styracosaurus* and *Centrosaurus* are thin, recurved, and unfused, but in the former the recurved morphology is retained into large adult size and the horncore never develops the procurved morphology common in *Centrosaurus*. The postorbital horncores of *Styracosaurus* are shorter and more rounded than those of *Centrosaurus* throughout ontogeny, and show greater resorption later in ontogeny. The length and thickness of the parietal processes increase drastically through ontogeny, but their position and orientation are static across the size series. Several diagnostic *Styracosaurus albertensis* specimens now preserve medially orientated P3 spikes, causing issues for the diagnosis of *S. ovatus*. Variability in parietal ornamentation, either expression of P1 and P2 parietal processes, or other cranial ornamentations, does not appear to correlate with stratigraphy.

## INTRODUCTION

*Styracosaurus* is an iconic centrosaurine ceratopsid dinosaur characterized by large, posteriorly and laterally projecting spike-like epiossifications on the posterolateral margins of the parietosquamosal frill (Lambe 1913; Ryan et al. 2007). It is stratigraphically restricted to the Campanian-aged upper Dinosaur Park Formation, 29–50 m above the contact with the underlying Oldman Formation (Ryan et al. 2007; Brown 2013). With the exception of three fragmentary skulls from the Two Medicine Formation of Montana (Gilmore 1930; McDonald 2011), it is also restricted geographically to the area within, or

close to, Dinosaur Provincial Park and Manyberries in southern Alberta. Although first described over 100 years ago (Lambe 1913), few representative specimens were known until relatively recently (Ryan et al. 2007; Holmes et al. 2020). Juvenile skulls of well-represented ceratopsid taxa are relatively rare, and with one notable exception (Currie et al. 2016) are either incomplete (Goodwin et al. 2006; Mallon et al. 2015) or are represented by isolated elements and specimens from monodominant bonebeds (Dodson and Currie 1988; Tokaryk 1997; Ryan 2007). Other putative juvenile ceratopsid material has been described (Gilmore 1917; Gilmore 1922; Dodson 1989), but these specimens have proven difficult to link to diagnostic

Published May 11, 2020

\*corresponding author. © 2020 by the authors; submitted February 18, 2020; revisions received April 22, 2020; accepted April 28, 2020. Handling editor: Jordan Mallon. DOI 10.18435/vamp29361

adult material, reducing their utility for studies of ontogeny (but see Penkalski and Dodson 1999; McDonald 2011). Sampson et al. (1997) and Frederickson and Tumarkin-Deratzian (2014) reviewed the craniofacial ontogeny of Centrosaurinae and *Centrosaurus*, respectively, but most of the available data for diagnostic material pertains to larger subadults and adults. As such, little is still known about the early ontogeny of the Ceratopsidae, including *Styracosaurus*.

One recently collected *Styracosaurus* specimen (TMP 2009.080.0001) comprises a nearly complete skull and partial postcranial skeleton. Comparison with other known specimens of *Styracosaurus* indicates that this specimen is the smallest, and likely youngest, essentially complete skull known for the genus. As such, it provides the opportunity to explore ontogeny and individual variation in this taxon, specifically the development of the cranial ornamentation, and to contrast these patterns with the better sampled close relative *Centrosaurus apertus*.

## MATERIALS AND METHODS

The specimen TMP 2009.080.0001 was examined at the Royal Tyrrell Museum of Palaeontology. The specimen consists of a nearly complete skull, a posterior cervical vertebra, two dorsal vertebrae, sacrum, two ribs and a scapulo-coracoid. Measurements were taken using digital and dial calipers (under 150 mm) and fiberglass measuring tape (over 150 mm; Tab. 1). Unless otherwise stated, measurements follow those of Ryan et al (2007). Photographs were taken using a Canon EOS 6D digital SLR camera with 50 mm [1:1.4] and 24–105 mm [1:4] lenses. Scientific line drawings were prepared from photographs. Dimensions were checked against the specimen, and then the final reconstructions were inked in using Koh-i-noor Rapidograph pens. Photographs were prepared into figures, i.e., removing backgrounds, assembling composite images, using Adobe Photoshop and Illustrator (CS5).

As part of a review of ontogeny and variation in the genus, all available diagnostic *Styracosaurus albertensis* material, particularly articulated skulls, parietosquamosal frills, and cranial material from monodominant bonebeds was examined. These materials were spread across five museums: Canadian Museum of Nature, Ottawa (CMN), Royal Alberta Museum, Edmonton (RAM), Royal Ontario Museum, Toronto (ROM), Royal Tyrrell Museum of Palaeontology, Drumheller and its Field Station in Dinosaur Provincial Park (TMP), and the University of Alberta Laboratory for Vertebrate Palaeontology, Edmonton (UALVP). One exception is a heavily reconstructed skull at the American Museum of Natural History (AMNH 5372), although additional cranial material (TMP 2006.019.0005) of this specimen – including parietal spikes collected in 2006 and 2015 – was

examined at the TMP. A full list of specimens is provided in Appendix 1. To quantify variability in the position and orientation of the serially homologous parietal spines, the position and orientation of each spike was measured in each reasonably complete parietal of *Styracosaurus*. The radial position of the base of each process along the margin of the parietal was measured by projecting a circular coordinate (compass) onto the centre of the fenestra (with 0° oriented medially, 90° oriented posteriorly, and 180° oriented laterally; Appendix 2). A radial coordinate system was chosen because this metric is independent of specimen size and robust to inconsistencies in the shape of the periphery of the parietal. The centre of the fenestra was approximated as the intersection point of the transverse line bisecting the fenestra at the anteroposterior midpoint, and a parasagittal line bisecting the fenestra at the transverse midpoint. Similarly, the orientation of the long axis (base to apex) of each spike was recorded using the same orientations (0° = medial, 90° = posterior, and 180° = lateral). All measurements were taken to the nearest degree using ImageJ (V 1.44) from dorsal images. Resulting data were plotted using R studio (V 3.4.3).

In addition to material of *Styracosaurus*, a large sample of the closely related (Ryan et al. 2012) species *Centrosaurus apertus* was also examined to provide a comparison with the cranial ontogeny in *Styracosaurus*. Specifically, an exhaustive sample of nasal horncores and postorbital horncores of *Centrosaurus apertus* from both articulated skulls and bonebed material, was examined (Appendix 3). A size series (based on basal size measurements) of *Centrosaurus* and *Styracosaurus* horncores in lateral views was created using Adobe Illustrator (CS5).

The assumed homologies of epiparietal follow those of Ryan (1992) and Sampson (1993; 1995) with epiossifications being numbered from medial to lateral. Under such a scheme a process projecting from the dorsal margin of the parietal, posterior to the fenestra, and curving anteriorly (if present) is designated P1, a process projecting from the posterior surface of the parietal and curving medial is designated P2, the medial most posterior spike is designated P3, and so on. For the squamosal, the epiossifications are numbered from anterior to posterior.

## GEOLOGICAL AND GEOGRAPHICAL CONTEXT

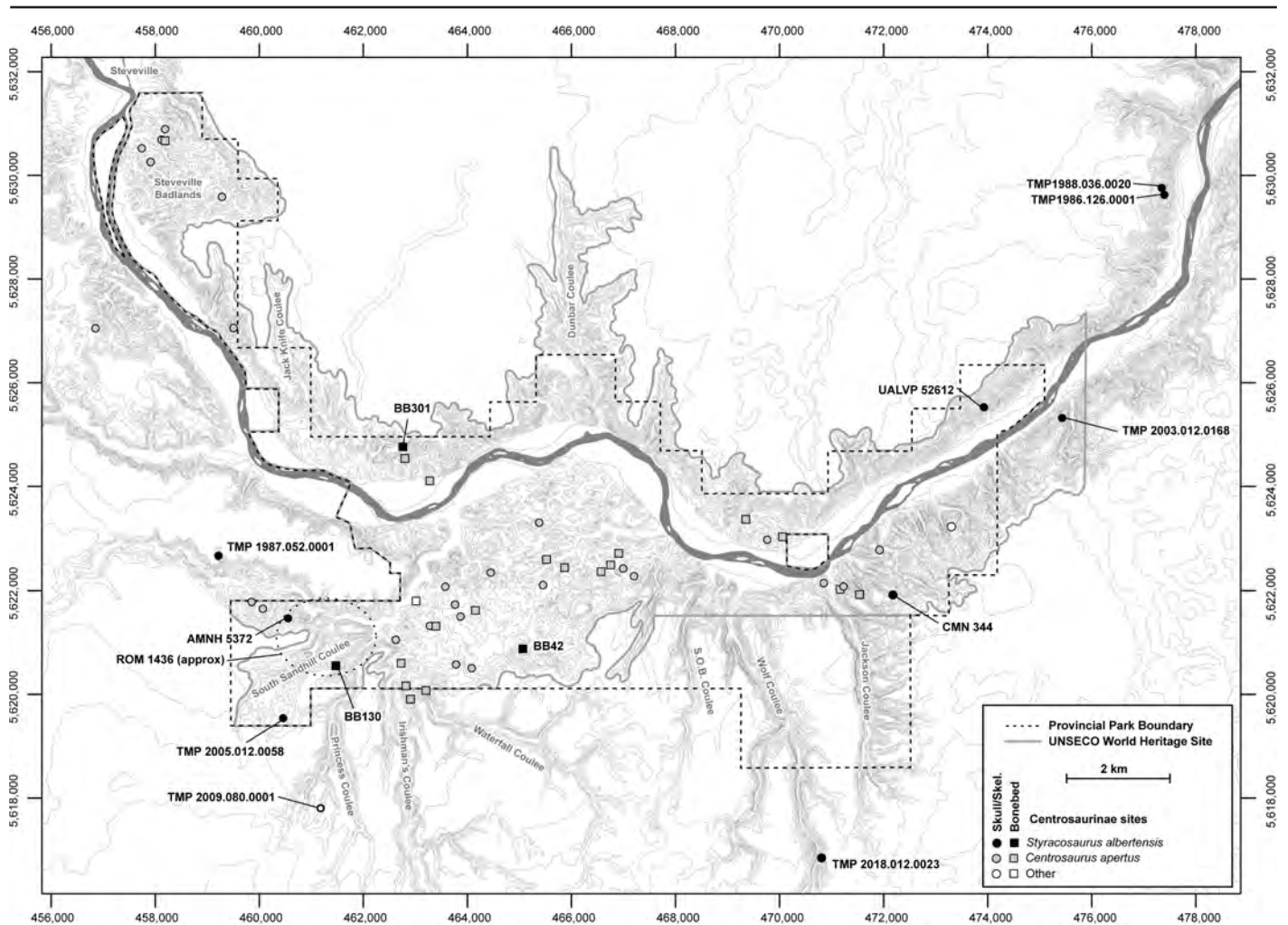
The *Styracosaurus* skull TMP 2009.080.0001 was found in August of 2008 and collected in August of 2009. The specimen was recovered from the upper (southern) portion of the central fork of Princess Coulee, just south of Dinosaur Provincial Park, Alberta (UTM; 12U, 461295 mE, 5617724 mN, 695.75 masl; Fig. 1), in the upper Dinosaur Park Formation (Campanian). The

Table 1. Measurements of *Styracosaurus* skull TMP 2009.080.001 following numbering from Ryan et al. 2007. Measurements in mm.

Dimension	Median	Left	Right
1 skull, midline length	1213 (no rostral)		
2 skull, total length	1435		
3 rostral-orbit length		540	530
4 rostral-posterior margin of nasal horncore	395		
5 rostral-back of tooth row		—	—
6 rostral-epijugal		710	660
7 interorbital width	320 (rt. Side X2)		
8 postorbital HC length		51	53
9 postorbital HC, antpost length		70	70
10 postorbital HC, Mediolateral width		40	37
11 orbit length		112	108
12 orbit, height		103	98
13 orbit, max diameter		120	126
14 post. margin of ext. naris-orbit		—	250
15 nasal horncore height	170		
16 nasal horncore basal length	133		
17 nasal horncore basal width	65		
18 jugal, minimal width		101	100
19 jugal-orbit length		—	238
20 lateral temporal fenestra-orbit		—	115
21 anterior margin of uto-parietal fenestra		—	214
22 squamosal, min. depth at medial sq. notch		196	—
23 squamosal caudal length		310	300
24 squamosal, caudal depth		270	270
25 ant. margin of pof. font-back of par. bar	620		
26 frontal fontanelle length	180		
27 frontal fontanelle, minimum width	60		
28 frontal fontanelle, depth	—		
29 parietal, total length	670		
30 parietal, midline bar length	440		
31 parietal, minimum ½ width		—	390
32 parietal, transv. width of midline bar (post. end)	148		
33 transv. ½ par. width to tip of P4	390		
34 transv. ½ par. width to tip of P6		—	458
35 parietal fenestra, max length		—	240
36 parietal fenestra, max width		—	230
37 transv. ½ par. width to notch between P5 and P6	390 (as in 31)		
38 basal length	690 (to back of lto – Scannella et al., 2014)		

Epiossifications	Length	Width	Thickness	Epiossifications	Length	Width	Thickness
S1 (left)	18	58	12	P3 (left)	—	91	41
S1 (right)	31	68	11*	P3 (right)	135 (18 mm lost)	85	30
S2 (left)	—	—	19	P4 (left)	—	114	29
S2 (right)	20	58	—	P4 (right)	130	75	30
S3 (left)	29*	73	18	P5 (left)	—	—	—
S3 (right)	22	62	—	P5 (right)	73	69	20
S4 (left)	21	69	15	P6 (left)	—	66	17
S4 (right)	23	55	—	P6 (right)	27 (from suture)	41	15
S5 (left)	—	—	—	P7 (left)	18	69	13
S5 (right)	—	—	—	P7 (right)	17	20	8
P1 (left)	—	—	27	P8 (right)	12	50	8
P1 (right)	26	83	34				
P2 (left)	—	—	25				
P2 (right)	—	—	—				

\*indicates best estimate



**Figure 1.** Map of Dinosaur Provincial Park, Alberta, illustrating the geographic localities of significant centrosaurine ceratopsid sites (quarries and bonebeds). *Styracosaurus albertensis* sites (black) are specifically labelled, while those of *Centrosaurus apertus* (grey) and other centrosaurines (white) (e.g., *Coronosaurus brinkmani*, 'c.f. *Pachyrhinosaurus*') are unlabelled. Circles indicate skulls and/or skeletons while squares indicate bonebeds. Hollow black circle is TMP 2009.080.0001. TMP 1989.097.0001 and UALVP 55900 are located outside of the mapped area. UTM Coordinates (Zone 12U) are indicated in the margin.

geographic position of the specimen in the upper reaches of the coulee system, just below prairie level, is similar to several other *Styracosaurus albertensis* specimens including AMNH 5372 and TMP 1987.052.0001 (Sandhill Creek), TMP 2005.012.0058 (South Sandhill Coulee) and TMP 2018.012.0023 (Wolf Coulee), or in the eastern portion of the main Red Deer River Valley (CMN 344, TMP 1986.126.0001, TMP 1988.036.0020, UALVP 52612), all of which represent outcrops of upper levels of the Dinosaur Park Formation. This is in contrast to the location of the majority of the *Centrosaurus apertus* quarries, which are found low in section within the Dinosaur Park Formation (Fig. 2), and are concentrated in the Core, Steveville Badlands, and main Red Deer River Valley (also known as Dead Lodge Canyon; Fig. 1).

The specimen was found at the base of a 4.5 m thick palaeochannel, 48 m above the contact between the Dinosaur Park Formation and underlying Oldman

Formation (Fig. 2). The host sandstone is characterized by inclined bedded sandstone with large to medium-scale trough crossbedding, carbonaceous drapes and a basal lag of ironstone clasts and fossils. The host sandstone overlies an organic rich mudstone and is in turn overlain by a marker shale (700.25 masl). The stratigraphic position of the specimen falls within the previously documented *Styracosaurus* zone (Ryan et al. 2007), but occurs fairly high in this zone, being one of the highest measured specimens in the Park area.

The specimen is a partial, disarticulated skeleton, with an articulated and nearly complete skull. The skull was positioned ventral side up with the left side of the parietal exposed to the midline, and the left squamosal eroding out of the rock. Several fragmented ribs were also exposed on the surface. The glenoid of the displaced scapulocoracoid was found hooked around the nasal horncore.

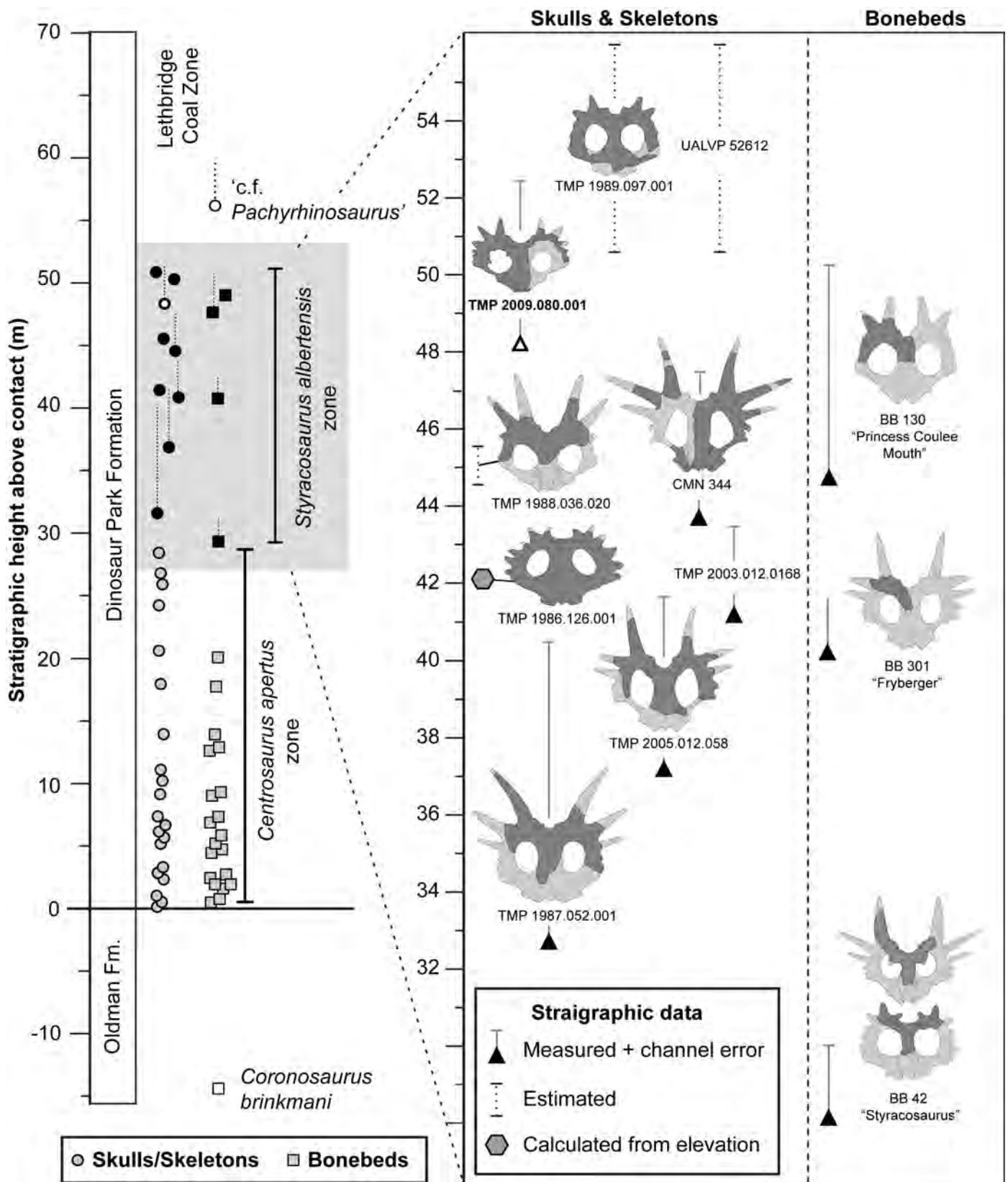


**Figure 2.** Stratigraphic position of *Styracosaurus albertensis* specimens within the Dinosaur Park Formation (Campanian) of Alberta, including both bonebeds and isolated skulls and skeletons. The column on the left shows the stratigraphic position of significant centrosaurine specimens, while the inset on the right highlights the parietal morphology of individual *Styracosaurus* specimens. Bonebeds samples show representative diagnostic specimen only (bottom to top: TMP 1999.055.0005, 1984.093.0001, 2016.015.0005, 2016.012.0029). Stratigraphic position is based on height above the Dinosaur Park/Oldman formation contact. Stratigraphic data derived from Brown (2013). Hollow circle and triangle indicate TMP 2009.080.0001.

## DESCRIPTION

The skull of TMP 2009.080.0001 has been prepared to expose the dorsal and lateral aspects; the ventral aspect is obscured by the supporting plaster jacket (Figs. 3–5). It is nearly complete with only the rostral bone and lower jaws missing. The associated right quadrate and quadratojugal became dissociated during burial (Fig. 6A, B), and were found appressed to the lateral surface of the squamosal; they have since been removed from the main skull block. The left half of the frill is broken into several pieces, but the lateral margins of both the left squamosal and parietal appear to be nearly complete and the bases of the parietal spikes are preserved in place (Figs. 3B, 5).

The palate and braincase are not exposed. However, the midline distance between the tip of the snout (missing the rostral) and transverse line drawn between the posterior margins of the lateral temporal openings, a proxy for basal length (Scannella et al. 2014), is 690 mm. Adding an additional 50 mm to accommodate the missing rostral still makes this individual, with an estimated basal length of 740 mm, the smallest nearly complete *Styracosaurus* skull known.

The right side of the skull is more complete and better preserved, although the squamosal has broken into two pieces and telescoped, and the dental ramus of the maxilla is obscured or more likely not preserved. Dorsoventral crushing of the skull has resulted in lateral splaying of the left half of the skull relative to the right, and as a result, the left side of the nasal bearing the posterior narial margin has rotated up and is visible in dorsal view (Fig. 3B). The left cheek, orbital region, and interorbital region have drifted as a unit a short distance laterally, and have rotated into the frontal plane. The jugal and squamosal are both broken, although the region of the lateral temporal opening is preserved.

### Snout

**Premaxilla:** The snout is relatively longer than in the holotype specimen (CMN 344). As a result, the nasal vestibule is distinctly longer than it is tall (Figs. 3A, 4A). Dorsally, the premaxilla is clasped by anterior processes of the nasal. The anterior margin of the premaxilla has broken away and has moved upward slightly. Otherwise, the snout is well-preserved and complete. The interpremaxillary suture had not fused in this region at the time of death (Fig. 4B). Although a dorsal portion of the internarial septum has broken away and become slightly displaced, it is still possible to determine the shapes and sizes of the septum and narial vestibules. As in other centrosaurines, the ventral (oral) margin of the premaxilla is strongly convex (Figs. 3A, 4A). The posteroventral process of the premaxilla is broad and spatulate with no posterior bifurcation. It reaches the lacrimal posteriorly, preventing the maxilla from making contact with the nasal. This condition is atypical for most

centrosaurines, but appears to be variable in *Centrosaurus*, and may be similarly variable in *Styracosaurus*.

**Maxilla:** Only the dorsal portion of the right maxilla is preserved; the inset, tooth-bearing ramus is obscured. It has slid slightly anteroventrally, exposing its underlapping surface with the jugal and displacing the trough-like anterior extension of the antorbital foramen ventrally. No tooth count or tooth row length can be determined.

**Nasal:** Anteriorly, the bifurcated anterior process of the nasal clasps the median posterodorsal process of the premaxilla (Fig. 3B). Immediately posterior to these premaxillary processes, the dorsal surface of the nasal is swollen and rugose and bears prominent grooves. Posterior to this, the nasal bears a pointed and distinctly posteriorly recurved horncore 170 mm tall (Figs. 3A, 4A). This thin and recurved morphology has been identified as juvenile morphology in *Centrosaurus* (Sampson et al. 1997; Frederickson and Tumarkin-Deratzian 2014). The lateral surface of the horncore is covered in distinct, largely longitudinal anastomosing grooves, the largest of these measuring ~140 mm long (82% total height) and 5 mm wide.

The horncore is laterally compressed and blade-like, such that the cross-section is an elongate oval with the minor (transverse) axis about 40% that of the major (antero-posterior) axis. This cross section is maintained along the height of the horncore, from the base (134 mm long, 55 mm wide) to the mid-height (85 mm long, 38 mm wide). Distinct, sharp ridges characterize the anterior and posterior extremes of the horncore along much of this length, but these become gradually rounded in the basal quarter. Despite its small size, the horncore shows no obvious external midline sutures, suggesting the left and right sides of the horncore are largely fused. This condition is also exhibited by a nasal horncore of nearly identical size and morphology (TMP 2009.031.0001; Fig. 7—specimen 55) collected from BB 301 (Fryberger *Styracosaurus* bonebed). In overall form, it also closely resembles the morphology of a very small, isolated, and unfused presumably juvenile horncore (TMP 1998.093.0163; Fig. 7—specimen 54; Ryan et al. 2007:fig. 8E, F, note this is incorrectly reported as TMP 1994.014.0866 in that caption), although it is more than twice the size (Tab. 1).

The nasal horncore is situated posterodorsal to the nasal vestibule, with most of the horncore posterior to, but the anteriormost third overlapping with, the nasal vestibule. Ventral to the horncore, the nasal forms the posterior margin of the nasal vestibule. The nasal appears to contribute to the septum, but a suture with the premaxilla cannot be identified. The narial process projecting from the posterior rim of the vestibule is distinctly inflected anteriorly into the vestibule.

### Circumorbital region

The two orbits are noticeably different in shape; the left orbit is nearly square with rounded corners (Fig. 5), and the right is distinctly longer measured along its posterodorsal-anteroventral axis than it is measured dorsoventrally (Figs. 3A, 4A) and oddly, the dimensions of the left and

right orbits are quite similar (Tab. 1, 11–13). Not all of this apparent difference can be accounted for by post-mortem distortion, indicating that there must have been some asymmetry in orbit shape during life. The orbits are relatively large, at 15 percent (average of all orbit dimensions) of basal skull length (Figs. 3A, 4A). Comparative relative

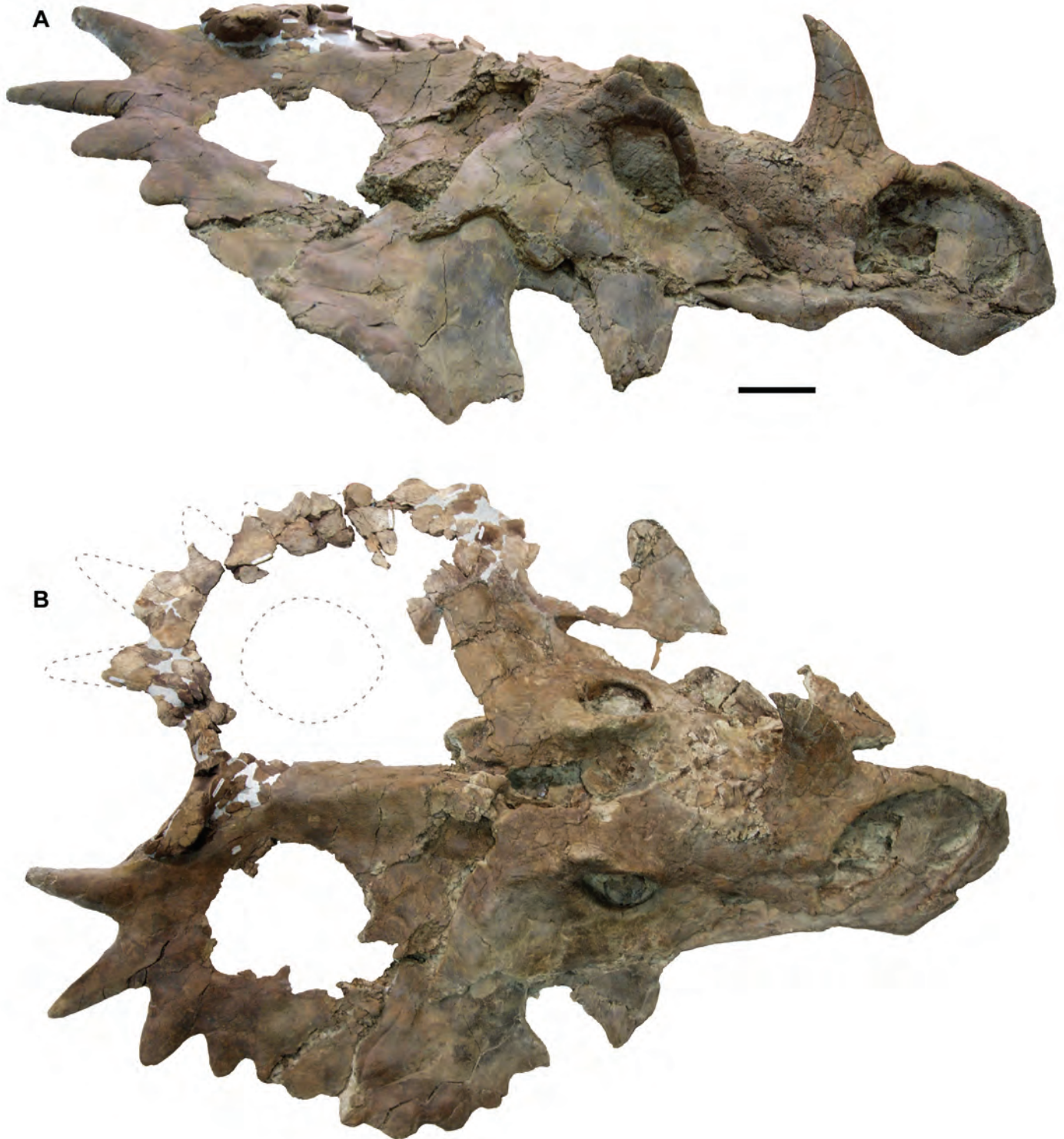


**Figure 3.** Right lateral (A) and dorsal (B) photographs of TMP 2009.080.0001, a subadult skull of the centrosaurine ceratopsid *Styracosaurus albertensis*. Dashed lines represent approximate extent of the left side of parietal. Scale bar = 10 cm.

orbit lengths for known, and presumed adult, *Centrosaurus* specimens average 13.5% (SD = 0.02, n = 14).

**Palpebral:** The palpebral forms the curved anterodorsal and dorsal margins of the orbit. It is well integrated into

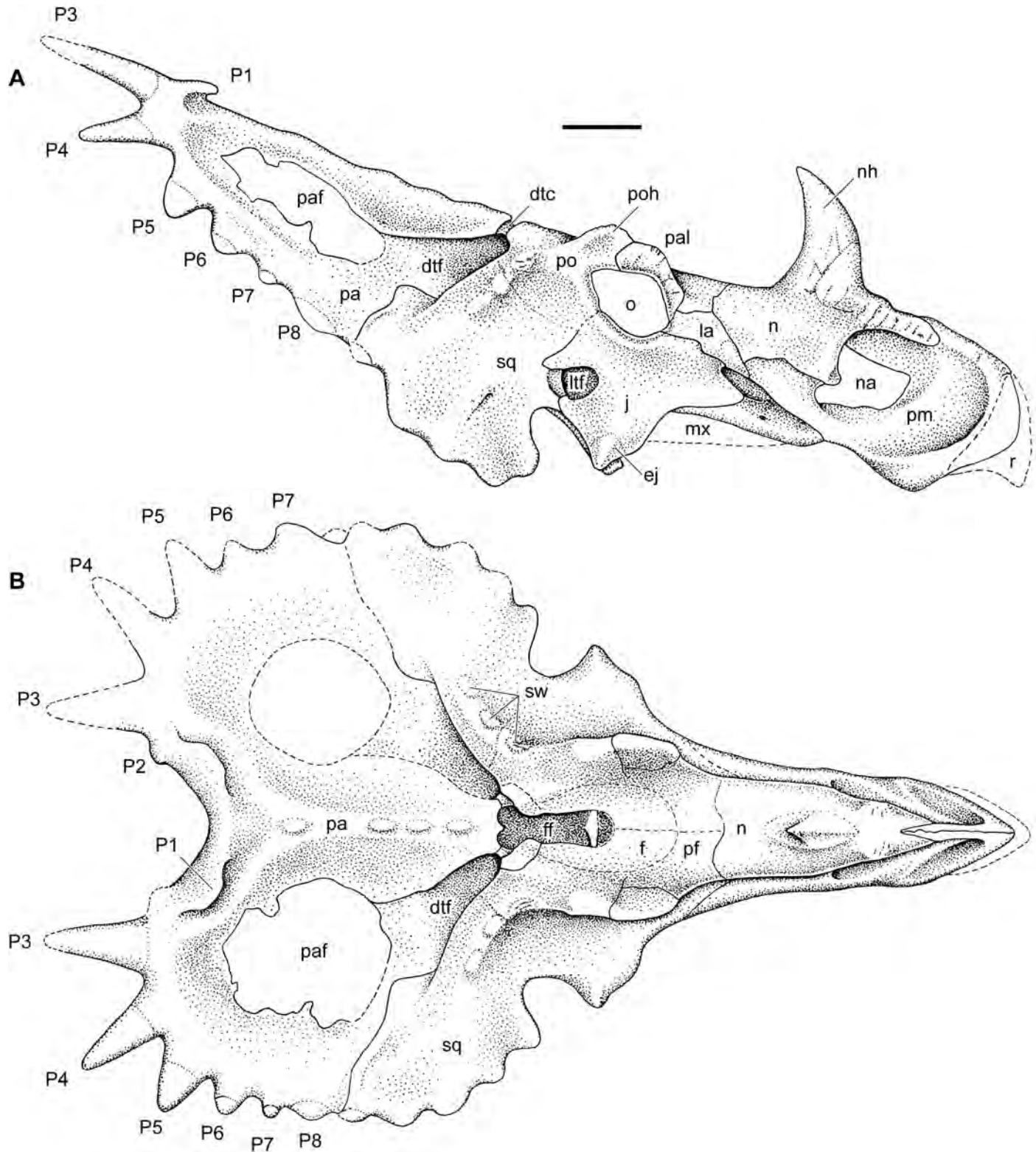


**Figure 4.** Right lateral (A) and dorsal (B) line drawings of TMP 2009.080.0001, a subadult skull of the centrosaurine ceratopsid *Styracosaurus albertensis*. Scale bar = 10 cm. Abbreviations: ej, epijugal (or facet); dtf, dorsotemporal fenestra; dtc, dorsotemporal channel; f, frontal; ff, frontoparietal fontanelle; j, jugal; la, lacrimal; ltf, laterotemporal fenestra; mx, maxilla; n, nasal; na, nasal ventibule; nh, nasal horncore; o, orbit; P#, parietal process; pa, parietal; paf, parietal fenestra; pal, palpebral; pf, prefrontal; pm, premaxilla; po, postorbital; poh, postorbital horncore; sq, squamosal; sw, swelling.

the skull, but traces of its sutures with the postorbital and prefrontal are still visible (Fig. 4). It bears a well-developed antorbital buttress with subtle radially oriented grooves on its flattened lateral face.

**Lacrimal:** The lacrimal is well integrated into the skull, but its sutures with the surrounding bones can be traced (Fig. 4A). It is elongated with a triangular anterior process. In contrast with most ceratopsids, the antorbital buttress

of the palpebral does not extend ventrally onto the lateral surface of the lacrimal.

**Prefrontal, Frontal:** The sutures between the frontals, prefrontals and nasals are quite well coossified, but the remaining traces allow their approximate courses to be reconstructed (Fig. 4B). Together, the frontal and prefrontal form the smooth, slightly arched skull roof from the posterior margin of the nasal to the anterior margin of the

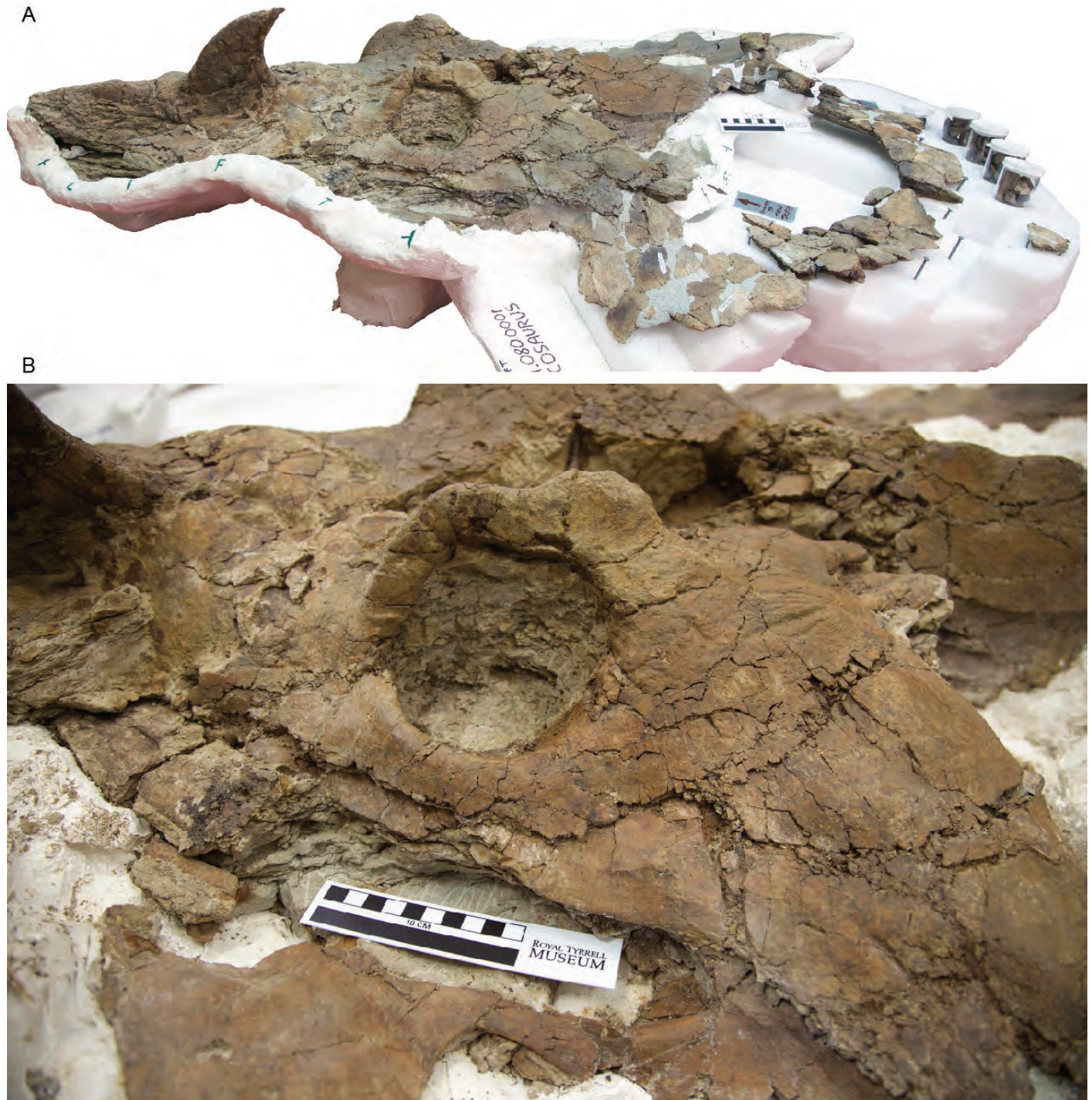


**Figure 5.** Photographs of the left side of TMP 2009.080.0001, a subadult of *Styracosaurus albertensis*, showing the overall skull (A) and an inset of orbital region (B). Scale bars = 10 cm.



**Figure 6.** Photographs of associated cranial and postcranial element of TMP 2009.080.0001. A & B, associated right quadrate and quadratojugal in lateral (A) and anterior (B) views. C–F, cervical vertebra (C5) in anterior (C), posterior (D), right lateral (E), and left lateral (F) views. G–I, dorsal vertebra in anterior (G), posterior (H) and left lateral (I) views. J, sacrum in ventral view. K–L, posterior left cervical rib in anterior (K) and posterior (L) views. M–N, partial left dorsal rib in posterior (M) and anterior (N) views. O–P, left scapulocoracoid in lateral (O) and medial (P) views. All scale bars = 10 cm. A–I & K–N, and J & O–P are at the same scale.

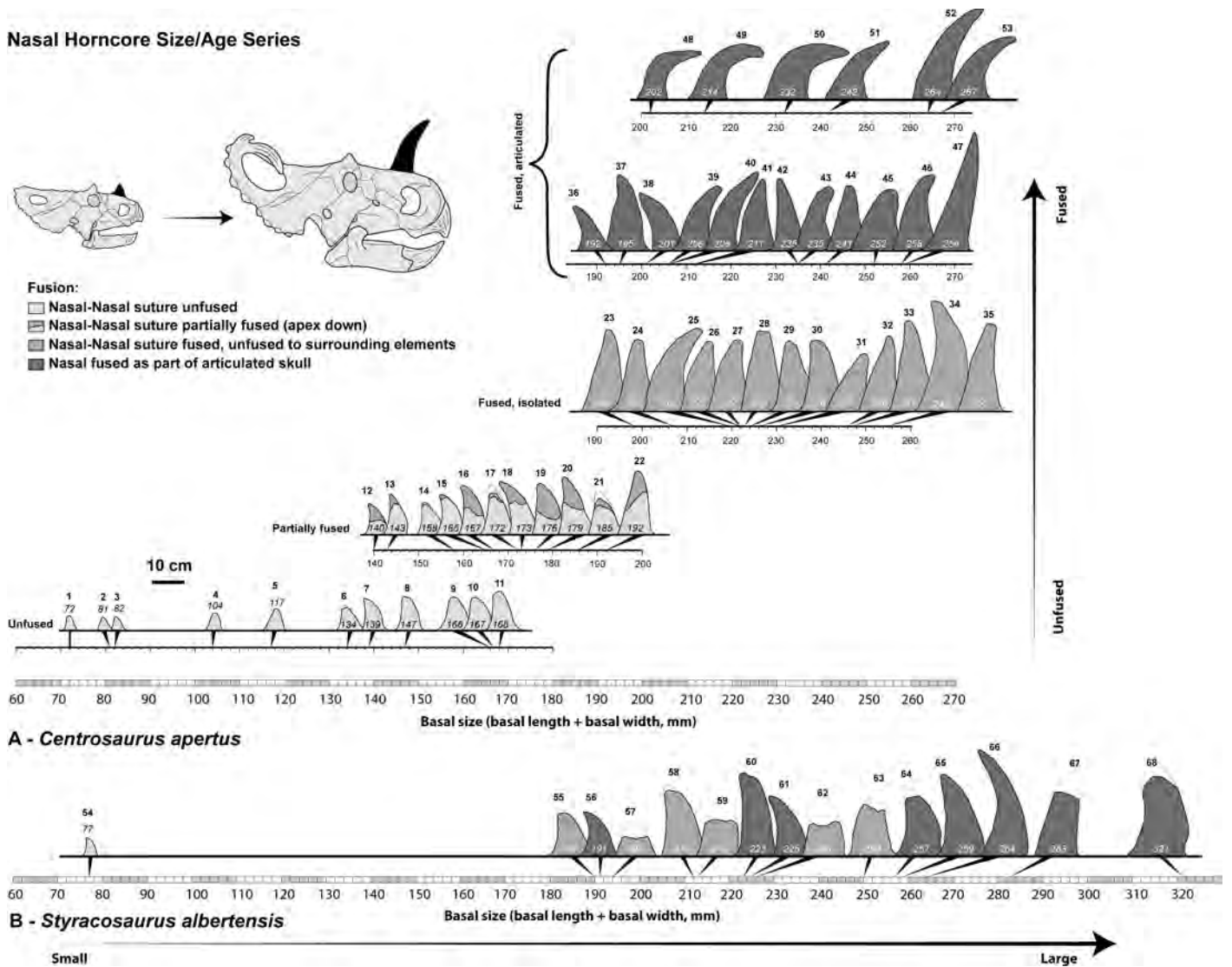


**Figure 7.** Size series of *Centrosaurus apertus* (A, upper) and *Styracosaurus albertensis* (B, lower) nasal horncores in right lateral view. Specimens are arranged along the horizontal axis according to their size (basal length plus basal width), and those of *Centrosaurus* are separated based on their degree of cranial sutural fusion (shaded infill). Although ordered based on size, the absolute position does not correlate directly with size due to spacing constraints. Numbers in italics indicate basal size metric, while numbers in bold refer to specimen numbers listed in Appendix 3.

frontoparietal fontanelle. Laterally they are bounded by the lacrimal, palpebral, and postorbital.

**Postorbital:** The postorbital forms the posterodorsal and posterior margins of the orbit and a short section of the anterior margin of the dorsotemporal opening. Immediately anterior to the latter opening, the postorbital bears a low, knob-like swelling traversed by anteroposteriorly oriented grooves (Fig. 4). A similar low knob is also seen in another partial *Styracosaurus* skull (TMP 2003.012.0168). The postorbital-squamosal suture appears not to have coossified at the time of death, at least on the better-preserved right side. The postorbital horncore is short (~50 mm, apex to orbital rim) and rounded dorsally with a slightly concave lateral surface resulting in an overall reniform morphology

in dorsal view, being ~70 mm long and ~40 mm wide (Figs. 3, 4). Its morphology is very similar to other individuals of comparable size/age both from *Styracosaurus* bonebeds (e.g., TMP 1966.010.0041; Fig. 8—specimen 105) and partial skulls (e.g., TMP 1986.126.0001). It bears some general similarity to smaller horncores described for juvenile *Centrosaurus* (Sampson et al. 1997; Ryan et al. 2007), but is quite unlike the tall, pointed and distinctly three-sided pyramidal horncores commonly present in *Centrosaurus* specimens of similar size. In contrast to other known *Styracosaurus* skulls (with the exception of TMP 1986.126.0001), the horncores show no distinct evidence of resorption pits. The apices of both horncores, however, bear small roughened patches that may represent incipient

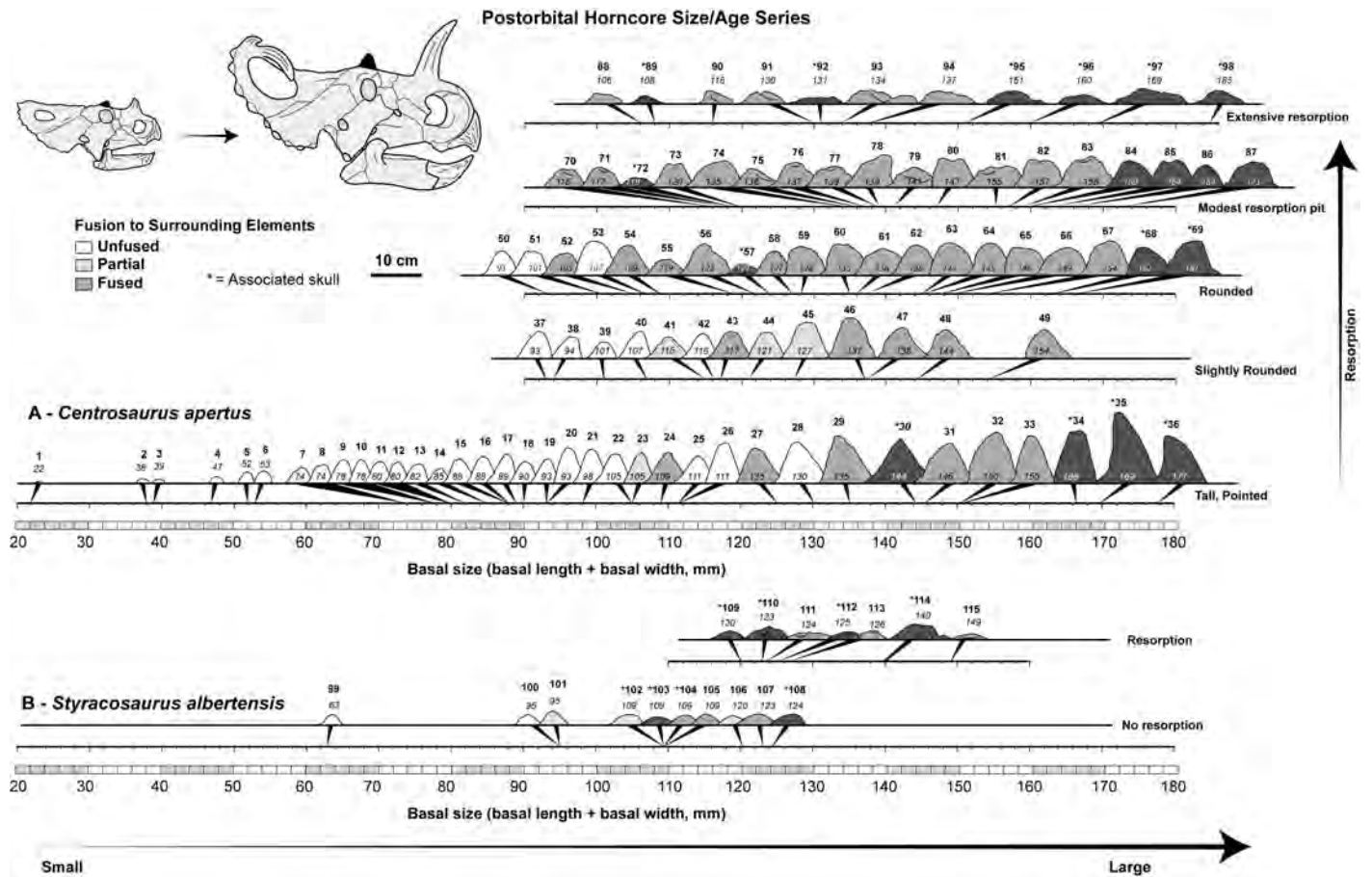


**Figure 8.** Size series of *Centrosaurus apertus* (A – upper) and *Styracosaurus albertensis* (B – lower) postorbital horncores in right lateral view. Specimens are arranged along the horizontal axis according to their size (basal length plus basal width), and separated vertically based on their degree of resorption. Although ordered based on size, the absolute position does not correlate directly with size due to spacing constraints. Numbers in italics indicate basal size metric, while numbers in bold refer to specimen numbers listed in Appendix 3.

resorption, or taphonomic damage, but lack the conspicuous longitudinal furrows and coarsely rugose texture seen in adult specimens of *Centrosaurus* and *Styracosaurus*.

**Jugal:** Both jugals are preserved. The right jugal overlaps the maxilla to form an oblique anterodorsally trending suture that extends far anteriorly. As a result, the jugal forms the superficial ventral margin of the antorbital foramen (Figs. 3A, 4A). This feature is unusual for centrosaurines, in which the jugal-maxillary suture is usually more vertical, and the jugal does not reach as far forward. This is variable in expression in *Centrosaurus*. Posterior to its suture with the maxilla, the jugal sweeps ventrally, and at its ventral tip swells laterally into a vertically inclined ridge bearing distinct rugosities. It is unclear if this swelling represents a fused, modestly sized epijugal ossification, or is merely the facet for one, the latter being more likely. This ambiguous anatomical interpretation makes it impossible to determine the precise size or shape of the epijugal. Disruption and telescoping of the right cheek have obscured the lateral temporal opening on that side, although its ventral margin is preserved. The left jugal pre-

serves the dorsal, anterior, and ventral margins of a large (approximately 54 mm in vertical dimension) lateral temporal opening. The bone has broken in two along a horizontal line about 30 mm below the orbit, and the ventral part has slid ventrolaterally about 50 mm. As a consequence, the jugal has become separated from its overlapping sutural connections with the squamosal immediately above and below the lateral temporal opening (Figs. 3B, 5).

**Quadrate/quadratojugal:** The nearly complete right quadrate and complete right quadratojugal are slightly disarticulated from each other, with the quadratojugal displaced posteromedial and dorsal relative to the quadrate, such that it is positioned posterior to the quadrate (Fig. 6A, B). The two elements had drifted away from their natural position onto the dorsal surface of the skull and were removed during preparation. The quadrate is missing its dorsal extremity, but the thin medial pterygoid wing is largely complete. This wing has a smaller ventrally positioned triangular projection, and a larger dorsally positioned rounded projection. Laterally the quadrate forms a rugose

butt-suture for the displaced quadratojugal, the ventral extreme of which is flattened and expanded into a triangular anterior process. Ventrally the quadrate swells to form the spool-like condyle. The medial and lateral swellings of the quadrate condyle are nearly equal in size and shape but the medial condyle extends slightly further ventrally. The displaced quadratojugal is wedge shaped, with broad, flattened sutural contact for the quadrate posteromedially and jugal anterolaterally. Only a thin wedge of quadratojugal would be exposed on the exterior surface of the skull. A triangular swelling projects from the posterolateral margin of the quadratojugal, and would be confluent with the swollen ventral margin of the jugal.

**Frontoparietal Fontanelle:** The right margin of the frontoparietal fontanelle appears to be complete except toward its anterior end (Figs. 3B, 4B). It is impossible to determine the exact size of the fontanelle because of the disruption and displacement on the left side of the skull, but appears to have been large, approximately 50 mm across at its widest point, and about 170 mm long. Near the anterior end of the fontanelle, the right side of a well-developed transverse buttress (Sternberg 1927) extends to the midline. The anterior extent of the fontanelle lies between the two postorbital horns. The floor of the fontanelle was shattered and largely lost post-mortem, so its original depth cannot be estimated with any confidence.

### Frill

**Squamosal:** Both squamosals are preserved, but only the right is complete (Fig. 3B). However, at some point during preservation, the latter broke into a dorsal portion (still articulated with the jugal and postorbital) and a ventral portion, and the latter then slid dorsomedially between 35–50 mm under the dorsal portion. A short process projects anteriorly below the lateral temporal fenestra to form a suture with the jugal, excluding the quadratojugal from forming any part of the ventral margin of the opening. The left squamosal bears the thickened, deeply bevelled posterior margin of the lateral temporal opening. Anterodorsal and anteroventral to the opening are the underlapping articular facets for the displaced jugal. The posterior part of the left squamosal is broken into several pieces, but its lateral edge appears to be almost complete. It bears a minimum of four episquamosal loci, although space is available along the poorly-preserved posterolateral aspect for a fifth; five may be a more accurate count. The more complete right squamosal bears four scalloped and gently convex episquamosal loci, but distinct episquamosals appear to be absent. A fifth epiossification straddles the lateral end of the squamosal-parietal suture (Figs. 3, 4). The main body of the squamosal is flat to slightly convex. Two low swellings are arranged diagonally across the element. More dorsally, two low swellings parallel the

anterior margin of the dorsotemporal opening and align with a third swelling on the postorbital.

**Parietal:** The parietal still retains its connections with both postorbitals, although the bridge underlying the left dorsotemporal channel that connects the frontoparietal fontanelle with the left dorsotemporal fenestra (Farke 2010) fractured and separated as the distal head of the median bar rotated counter clockwise about 25 degrees. The median, anterior projection of the median bar is preserved (Figs. 3B, 4B). In both its overall morphology, and the frill ornamentation, the parietal of TMP 2009.080.0001 is most similar to that of another small *Styracosaurus* specimen TMP 1987.097.0001. The median bar is wide, with slightly concave dorsolaterally facing sides rising steeply to form a wedge-shaped median ridge. A prominent median ridge is characteristic of protoceratopsids. A similar morphology is also present in TMP 1986.126.0001, another small skull, but is not seen in larger *Styracosaurus* skulls, where the bar is broadly rounded dorsally. The same ontogenetic trends have been noted in *Centrosaurus* (Sampson et al. 1997; Frederickson and Tumarkin-Deratzian 2014) and chasmosaurines (Currie et al. 2016). Posterior to the midpoint of the bar, the median ridge becomes more gently rounded. The ridge bears three prominent lenticular knobs anteriorly, and a slightly less conspicuous knob more posteriorly – these are also much less prominent in larger skulls (e.g., CMN 344, UALVP 55900). The right parietal fenestra is roughly oval in shape, with the long axis oriented anterolaterally (Figs. 3B, 4B). Its margin is highly irregular. It is unlikely that this simply reflects damage and loss of bone, as the right half of the frill is otherwise well preserved. It is more likely that, as in UALVP 55900 (Holmes et al. 2020), the bone had not ossified sufficiently to form a smoothly curved fenestral border. The lateral fenestral margin is interrupted by a distinct triangular wedge of bone (35 mm long) projecting from the lateral parietal bar into the centre of the fenestra. This morphology is seen on some *Centrosaurus* specimens (e.g., CMN 8798), but other than UALVP 55900 (Holmes et al. 2020) has not been reported in *Styracosaurus*.

Both P1 epiossifications are preserved, but the right, upon which the following description is based, is much more complete (Figs. 3B, 4B). It is broad-based but short. Unlike the holotype (CMN 344), it is distinctly procurved. However, unlike some *Styracosaurus* specimens (Ryan et al. 2007; Holmes et al. 2020: figs. 9, 14), it is squared off in dorsal view rather than triangular. Immediately anterior to its base, the dorsal surface of the parietal bears a shallow sulcus. The left P2 is relatively prominent, but is triangular to tab-like in outline rather than hook-like as in ROM 1436, TMP 1986.126.0001 (Ryan et al. 2007: figs. 13, 14), and UALVP 55900 (Holmes et al. 2020). The right P2 is not

preserved, but its base can be identified immediately medial to the right P3. Six additional epiparietals are preserved on the right parietal (Figs. 3B, 4B). Parietal processes at P3 and P4 are straight, triangular, spike-like, and are slightly dorsoventrally compressed with oval cross-sections. The apex of P3 is incomplete; based on the shape of the preserved portion, about 18 mm of its tip is missing, making it the longest of the series (Tab. 1). Unlike the holotype, it projects posteriorly and slightly medially. The complete, posterolaterally projecting P4 is slightly shorter than the estimated total length of P3, but otherwise of similar morphology. Processes at loci P5 and P6 are also triangular, but progressively shorter than P4, and more dorsoventrally compressed, with P5 being approximately as long as wide. Epiparietal 7 is more knob-like and much less well coossified with the parietal than the other epiparietals. The process at P8 is fully 'D'-shaped in outline, and indistinguishable from the homologous ossification of *Centrosaurus*. The left parietal is not as well preserved, but appears to be similar to the right side. The lateral parietal processes on the left are similar in morphology to those on the right, with a few minor exceptions. On the left side, the base of P4 is larger than that of P3, the reverse of the situation on the right. In addition, the epioossification count on the left is less than the right, with only seven loci. It is uncertain whether a transitional ossification spanning the parietal-squamosal suture was present. This suggests at least some asymmetry in the parietal ornamentation. Unlike some centrosaurines (e.g., *Sinoceratops* – Zhucheng Dinosaur Museum V0010, *Wendiceratops* – TMP 2011.051.0009, 2014.029.0097), none of the lateral epioossifications curve dorsally/anteriorly. As in the holotype, their bases are in the plane of the frill, and distally curve slightly ventrally. There is little or no indication of imbrication.

## Postcranial skeleton

**Vertebrae:** Specimen TMP 2009.080.0001 includes three presacral vertebrae and the sacrum. The best preserved presacral vertebra is a posterior cervical (Fig. 6C–F). The anterior and posterior facet of the centrum is slightly heart-shaped (Fig. 6C), with a distinct parapophysis positioned on its lateral-most surface, slightly dorsal to the midpoint (Fig. 6E, F). Its centrum is 114 mm in transverse diameter (width), 50 mm in length, and 91 mm in vertical diameter (height). The neural canal is relatively large (31 mm wide, 29 mm tall) and a rounded triangle in shape, with the apex directed dorsally. The transverse processes are directed laterally in the horizontal plane and are in line with the dorsal extent of the neural canal. The triangular, dorsally tapering neural spine is 53 mm tall, orientated vertically, and has a transverse expansion at its dorsal apex. The pre- and postzygapophyses arise from the anterior and posterior bases of the neural spine dorsal to the transverse processes. A thin

midline ridge, a ventral continuation of the neural spine, separates the prezygapophyses, while a reciprocal midline notch separates the postzygapophyses. The oval postzygapophyseal facets lie at  $\sim 45^\circ$  to the horizontal, while those of the prezygapophyses are steeper at  $\sim 60^\circ$ . In morphology, this vertebra closely matches the fifth, or possibly sixth, cervical vertebra (second and third free cervicals) in the holotype of *Styracosaurus* (CMN 344: Holmes and Ryan 2013). The total height of the vertebra is 210 mm, and the width between transverse processes is 158 mm. While the centrum width is of similar size to the homologous element in the holotype specimen (CMN 344), other measures are smaller (Holmes and Ryan 2013). Neurocentral synchondroses are fused on this and all other known vertebrae of the specimen.

A posterior trunk vertebra is more poorly preserved, with its centrum badly crushed and much of its external surfaces lost (Fig. 6G–I). As a result, it is difficult to determine its dimensions. No distinct parapophysis is observed, but given the condition of the bone this may be obscured. The preserved portion of the centrum appears to be oval in anterior and posterior views, taller than wide, with a preserved transverse diameter (width) of 99 mm, and vertical diameter (height) that is incomplete. Due to crushing, the centrum length cannot be determined. The neural canal is oval in shape, 25 mm wide and 32 mm tall. The transverse processes project dorsolaterally at an angle of  $\sim 45^\circ$  to the horizontal, and are only slightly posteriorly inclined. Although the left process is incomplete, the transverse distance between the apices would have been  $\sim 200$  mm. The prezygapophyses are positioned in line with the base of the transverse processes, while the postzygapophyses are located further dorsally. The circular to oval facets of both the pre- and postzygapophyses lay at  $\sim 45^\circ$  to the horizontal. The neural spine is tall (84 mm), rectangular, and slightly posteriorly inclined. The total height of the vertebra is estimated at  $\sim 254$  mm.

A second dorsal vertebra is also present, but it is poorly preserved with most of its surface lost, and cannot be identified with confidence. Both the centrum and the neural canal are taller than wide, and the arch is taller and more constricted than the previously described dorsal. Further details cannot be determined.

The nearly complete synsacrum has been described previously (Holmes and Ryan 2013). It is prepared in its field jacket, such that only the ventral surface is exposed (Fig. 8J). The synsacrum is composed of an ankylosed series of two dorsosacrals, four true sacrals and two caudosacrals with a total length of 662 mm. The dorsosacral centra have the greatest transverse widths, with the anterior of the two measuring 149 mm, and the posterior 169 mm. In contrast, the first sacral centrum is an isosceles trapezoid, with a broad anterior width (140 mm) and greatly constricted

posterior width (104 mm). The remaining sacral centra are narrow (85–67 mm in an anteroposterior sequence) and spool shaped. The second caudosacral is transversely wider (109 mm) than the first (70 mm). The ventral surfaces of the two dorsosacrals and first two sacrals are relatively flat, with a shallow medial groove, whereas the centra of the remaining sacrals and first caudosacral form a continuous midventral keel. The synsacrum supports six broad based sacral ribs, the anteriormost anchoring from the posterolateral margin of the last dorsosacral and the anterolateral margin of the first sacral (S1), and the posteriormost anchoring from the posterolateral margin of the first caudosacral and anterolateral margin of the second caudosacral. Laterally the sacral ribs expand anteroposteriorly to form a contiguous, crescentic acetabular buttress and iliac facet 381 mm long. The anteriormost sacral rib is the longest (172 mm) whereas the lengths of the ribs gradually decrease to the fourth (87 mm), and increase again to the sixth (112 mm).

**Ribs:** Two left ribs are preserved. One has a straight shaft and widely separated proximal articulations (although the parapophysis is largely missing) identifying it as a posterior cervical (Fig. 6K, L). The shaft, missing only the distal extremity, measures 396 mm in preserved length. It is largely circular in cross-section, with a midpoint diameter of 19 mm. The other rib is larger, with a flat, curved shaft, and lacks the proximal end (Fig. 6M, N). However, its large size identifies it as an anterior trunk rib. It is oval in cross-section with an anteroposterior diameter of 39 mm, and a transverse diameter of 13 mm.

**Scapulacorocoid:** A complete left scapulacoracoid is preserved (Fig. 6O, P), and was closely associated with the skull – as preserved the glenoid was hooked around the nasal horncore. The entire unit is 798 mm long, with the scapula being 663 mm long. The greatest width of the scapula is 212 mm, while the minimum width, located at midshaft, is 102 mm. The two elements are well fused, such that the dorsal portion of their suture is difficult to demarcate. The coracoid is ~305 mm long and 174 mm in maximum width, and bears a distinct coracoid foramen, the fossa of which is ~30 mm in diameter. The coracoid is characterized by a crescentic anterior margin, which shows a distinct medial folding, a ventral margin with a hook-like ventral process (90 mm long) anteriorly and glenoid fossa posterior, and a relatively straight posterior margin fused to the scapula. The glenoid fossa is 145 mm long, 65 mm in maximum thickness, and nearly equally bisected by the scapulacoracoid suture, with the scapula contributing only slightly more to the glenoid than the coracoid. The shaft of the scapula is rectangular with a distinct dorsoventral expansion at its anterior, and to a lesser extent, posterior extremes. The lateral surface of the scapula is dominated by

the round scapular spine, which traverses from the anteroventral margin (posterior margin of the glenoid) diagonally across the element to flatten out near the posterodorsal margin. Medially, the scapula is flat. The posterior margin of the scapula is incomplete, but square, and only slightly expanded in thickness.

In both size and morphology, the scapulacoracoid closely matches that of TMP 1989.098.0001, another small *Styracosaurus*, with both being ~85% the length of the holotype (CMN 344). In contrast with the larger holotype, the two smaller specimens (TMP 2009.080.0001 and 1989.098.0001) show a less distinct and less swollen margin around the glenoid fossa, a less developed anterior crescentic margin of the coracoid, and posterior region of the scapular shaft that is less expanded.

## DISCUSSION

**Immature status of TMP 2009.080.0001.** Several size-independent features on the skull suggest that TMP 2009.080.0001 is ontogenetically young and not representative of the standard adult *Styracosaurus* condition. Many of these features are consistent with known patterns of craniofacial ontogeny in Centrosaurinae (Sampson et al. 1997) and *Centrosaurus* (Frederickson and Tumarkin-Deratzian 2014), and some have been documented previously for *Styracosaurus* (Ryan et al. 2007). The midline intermaxillary suture is open in anterior view (Frederickson and Tumarkin-Deratzian 2014, char. 12:0). The nasal horncore is small (char. 15:0), laterally compressed and blade-like (char. 17:0), and is recurved (char. 13:0). The palpebral-postorbital suture is only partially obscured (char. 41:1). The postorbital horncore is low and rounded (char. 37:0), lacks any indication of resorption pits (char. 32:0), and is not dominated by a rugose texture (char. 36:0). All squamosal epiossification sutures are open (in fact, no squamosal epiossifications are present) (char. 48–51:0). Although the parietal fenestrae fall above the 50% sagittal length threshold for the juvenile character state in (Frederickson and Tumarkin-Deratzian 2014, char. 58:1), they are relatively small. The posterior and lateral parietal bars are thin (char. 72:0).

In addition to the ontogenetic characters identified by Frederickson and Tumarkin-Deratzian (2014), there are several other features indicating the specimen may be a young animal. The median bar of the parietal is triangular in cross section, and bears a pronounced, acuminate dorsal median ridge, similar to TMP 1986.126.0001 but in contrast with larger specimens where this ridge is broadly rounded. Additionally, the lateral epiossification loci are inline (i.e., not imbricated), the orbit is relatively large (orbit size is negatively allometric in vertebrates), and the antorbital buttress of the palpebral does not extend onto the lacrimal.

Although the skull of TMP 2009.080.0001 exhibits many immature features, distinct long-grain and mottled bone textures (Frederickson and Tumarkin-Deratzian, 2014; char. 9, 30, 56, 80), which are good size independent indicators of relatively young age in Centrosaurinae (Sampson et al. 1997; Brown et al. 2009; Tumarkin-Deratzian 2010), are entirely absent. Rather, the surficial bone texture is more consistent with a subtle adult texture. This absence of long-grained and mottled bone textures is not easily attributed to taphonomic damage as the specimen shows distinct bone textures elsewhere, and other bonebed derived specimens show these distinct textures even when the elements have been subject to higher degrees of abrasion and damage. Nevertheless, the short, triangular, and dorsoventrally compressed morphology of P3 and P4 in TMP 2009.080.0001 closely matches that of other, presumed subadult material of *Styracosaurus*, both from BB42 (e.g., TMP 1981.019.0223, TMP 1995.055.0005) and isolated skulls (e.g., TMP 1997.012.0122), all of which do show long-grained and mottled textures. This suggests TMP 2009.080.0001 may only just have lost the mottled textures seen on these specimens. The loss of these textures in *Centrosaurus* is correlated with the development of the parietal ornamentation (Brown et al. 2009), so their absence in this skull, with small but diagnostic ornamentation is not surprising.

Based on the suite of character states, it is likely the specimen had not achieved skeletal maturity. However, the skull, with a basal length of about 740 mm, is relatively large, ~90% the length of the holotype (CMN 344) and ~80% the length of the recently described UAVLP 55900. Similarly, the scapula of TMP 2009.080.0001 is 663 mm long, ~85% the size of CMN 344, and nearly identical in size to TMP 1989.097.0001 (Fig. 9). Following the definition of Sampson et al. (1997), the specimen is therefore referred to as a subadult, as opposed to a juvenile, because it has attained a body size approaching that of large, adult specimens, but retains several immature features.

Despite its relatively large size, the cranial ornaments are poorly developed. The nasal horncore is less than one-third the height of the holotype specimen (CMN 344—reconstructed), while the parietal processes P3, P4 and P5, are all only slightly greater than one-quarter their counterparts in the holotype. A nearly identical pattern is seen in TMP 1989.097.0001, which, based on postcranial measurements is ~80% the size of the holotype (see Holmes and Ryan 2013), yet bears parietal processes approximately ~25% of the size of those of the holotype (Fig. 9). Together these results suggest that the sizes/expression of the cranial ornaments in *Styracosaurus* are strongly developmentally delayed, and disconnected from overall skeletal size, such that they do not develop until the individual is near adult size. These results are consistent with previous hypotheses

regarding the timing of development of cranial ornaments in Centrosaurinae (Sampson et al. 1997), as well as Hadrosauridae (Evans 2007; Evans 2010; though see Farke et al. 2013), and are consistent with the interpretation of these features evolving in the context of sociosexual selection.

**Ontogeny of Cranial Ornaments in *Styracosaurus*, and Comparison with *Centrosaurus*.** Although many of the ontogenetic characters well established for Centrosaurinae and *Centrosaurus* (Sampson et al. 1997; Frederickson and Tumarkin-Deratzian 2014) appear to be reflected in the ontogeny of *Styracosaurus*, until recently the restricted sample size in the latter made it difficult to evaluate this impression. The recent discovery of several new specimens, in particular TMP 2009.080.0001, now allows for direct comparison between the two taxa, specifically with respect to development of the cranial ornaments.

**Nasal:** Figure 7 depicts a size series, and hypothesized growth series (although size is not an exact proxy of age), of both *Centrosaurus* and *Styracosaurus* nasal horncores constructed using an extensive sample of both articulated skulls and bonebed material. In *Centrosaurus*, nasal horncore ontogeny progresses from small, equilateral, and unfused forms (Fig. 7, specimens 1–5), through distinctly posteriorly recurved forms with fusion from the apex towards the base (specimens 8–22), into large, fully-fused forms ranging from straight (specimens 23–35), to slightly (specimens 36–47), and strongly (specimens 48–53) anteriorly procurved (Fig. 7A). While exceptions exist (e.g., specimens 36—TMP 1992.082.0001, 38—CMN 8798) and variability in the size/shape at fusion is seen (e.g., specimens 9, 10, 11 vs. 12, 13), this pattern is both fairly constrained and largely correlated with basal sizes of the horncores and estimated sizes of the individuals.

In *Styracosaurus* the pattern is similar (Fig. 7B), but with several notable differences. At the smallest size (specimens 1—TMP 1995.400.0074 for *Centrosaurus*, 54—TMP 1998.093.0163 for *Styracosaurus*) the two taxa cannot be differentiated, but potential differences are seen as the nasals begin to fuse. Despite the many immature features of the nasal horncore in TMP 2009.080.0001, the nasal-nasal suture in the horncore appears to be fully fused (char. 20:3 of Frederickson and Tumarkin-Deratzian 2014). This is in contrast to the pattern in *Centrosaurus*, where specimens of similar small size and thin, recurved morphology are generally only partially fused (Fig. 6). TMP 2009.080.0001 (specimen 56) is not unique, as a nearly identical morphology is preserved in a nasal from a *Styracosaurus* bonebed (specimen 55—TMP 2009.031.0001). Together, these suggest that the paired nasals of *Styracosaurus* may have fused at a smaller/younger stage than in *Centrosaurus*. Also, in contrast with *Centrosaurus*, fused nasals of *Styracosaurus* largely retain the juvenile condition of being posteriorly

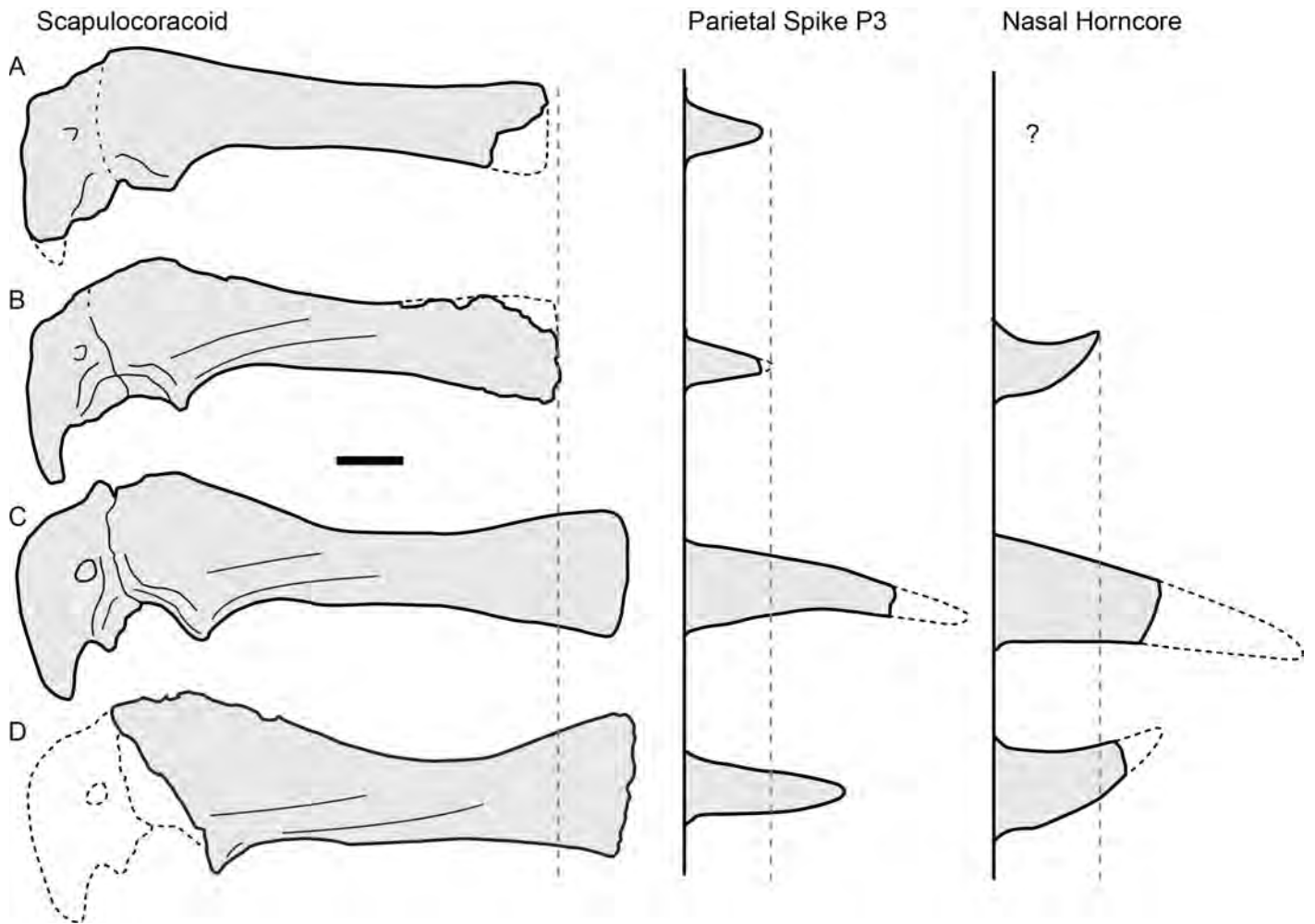


**Figure 9.** Absolute size comparison between the scapulocoracoid in lateral view (left column), parietal spike P3 in dorsal view (central column), and nasal horncore in left lateral view (right column) for four *Styracosaurus* specimens. A, TMP 1989.097.0001 (subadult). B, TMP 2009.080.0001 (subadult). C, CMN 344 (adult). D, UALVP 55900 (adult). All elements scaled to the same size. Scale bar = 10 cm.

recurved or, at the most, straight (specimen 67—CMN 344) regardless of the absolute size of the horncore. In this way *Styracosaurus* horncore morphology mirrors an early ontogenetic stage of that of *Centrosaurus*, and may represent an example of paedomorphosis, despite the apparent early fusion of the element. Whether or not the fusion at a smaller/earlier growth stage is related to the less variable curvature of the nasal horncore in adults is unclear, but it remains a possibility. As the procurved morphology in *Centrosaurus* is restricted to fully fused nasals, and largely associated with articulated skulls, it may be that early fusion in *Styracosaurus* constrains this morphology.

Despite the possibility that horncore shape in *Styracosaurus* is paedomorphic relative to *Centrosaurus*, the maximum size of *Styracosaurus* nasal horncores greatly exceeds that of *Centrosaurus* (Fig. 7). This represents an interesting juxtaposition in horncore shape versus horncore size between these two closely related animals, where *Styracosaurus* adults have the nasal horncore morphology of juvenile/subadult *Centrosaurus*, but are much larger in absolute size.

**Postorbital:** Figure 8, constructed using both articulated skulls and bonebed material, represents a size series, and hypothesized growth series, of both *Centrosaurus* and *Styracosaurus* postorbital horncores. In *Centrosaurus* postorbital horncore ontogeny progresses from small, laterally compressed hemispherical horncores (Fig. 8, specimens 1–6) to tall, three-sided, and pointed-apex horncores that remain unfused to the surrounding elements (specimens 7–22; Fig. 8A). Fusion with the palpebral and associated elements is accompanied or followed by resorption of the horncore, from slight (specimens 37–49) to increasing (specimens 50–69) roundedness of the apex, development of a distinct resorption pit (specimens 70–87), and nearly complete resorption (specimens 88–98). Several exceptions to this pattern exist, with some horncores showing no resorption, and retaining a tall, pointed-apex morphology to large size (specimens 29–36). There is also a great deal of variation across the size series with respect to where/when fusion and resorption occurred.

The postorbital horncores of *Styracosaurus* are distinct from *Centrosaurus*, even at the smallest comparable sizes (Fig. 8B). The smallest *Styracosaurus* postorbital horncore (specimen 99—TMP 2014.15.0084) is a low rounded dome, longer than tall. This is in sharp contrast to horncores with similarly sized bases in *Centrosaurus* (e.g., specimens 7—TMP1979.011.0117 and 8—TMP 1981.022.0013), which are twice as tall and have pointed apices. Postorbital horncores consistently remain short through the entire size series in *Styracosaurus*, with no specimen developing the tall pointed morphology, regardless of size (Fig. 8B). The postorbital horncores of TMP 2009.080.0001 (specimen 102) differ from the classic ‘pyramidal’ horncores representative of subadult *Centrosaurus* (e.g., specimens 22—TMP 1982.018.0017, 23—TMP2015.059.0023, 24—TMP1998.093.0034) in that they are low (half the height of similarly sized horncores in *Centrosaurus*) with rounded apices and concave lateral surfaces. This morphology is not unique to TMP 2009.080.0001, but is seen in several other bonebed and articulated specimens (e.g., specimens 103—TMP 1986.126.0001, 104—TMP1966.010.0041). At the extreme end of the size series, *Styracosaurus* does show extensive resorption (e.g., specimens 109–115) similar to *Centrosaurus* (specimens 89–98), with a complete lack of discrete horncores in many cases. At this stage, the two taxa are largely indistinguishable. One potential difference, however, is that these resorbed horncores of *Styracosaurus* have smaller basal sizes than in *Centrosaurus*, another indication that the postorbital horncores in *Styracosaurus* are truncated, as they do not reach as large a size as in *Centrosaurus*. A second distinction, based on the current sample, is that a majority of fused *Styracosaurus* postorbitals show extensively resorbed conditions. This is in contrast to the *Centrosaurus* sample in which fewer than a third show this condition. It is unclear if these two distinctions are due to sampling differences, taphonomic bias, as a result of *Styracosaurus* postorbital horncores being absolutely smaller (i.e., having less to resorb), or being resorbed at an earlier stage relative to *Centrosaurus*.

It is worth noting the apparent reciprocal ontogenetic trajectories between the nasal and postorbital horncores. Relative to *Centrosaurus*, *Styracosaurus* nasals are larger but exhibit a juvenile morphology, while *Styracosaurus* postorbitals are generally smaller and show higher levels of resorption.

**Parietal:** Figure 10 shows the variation, both ontogenetic and likely independent of ontogeny, across all known relatively complete parietals of *Styracosaurus*.

Parietal morphology does change dramatically through ontogeny, with those features showing the most dramatic changes being the sizes and shapes of the parietal processes,

specifically their apical-basal lengths, dorsoventral thicknesses, and basal circumferences (Fig. 10). Smaller, presumably subadult individuals (e.g., TMP 1989.098.0001 and TMP 2009.080.0001) bear short, thin (dorsoventrally compressed) and triangular parietal processes, while larger, presumably more mature skulls (e.g., CMN 344, TMP 1987.052.0001, 2005.012.0058, ROM 1436, and UALVP 55900) bear thick, rounded in cross section and spike-like parietal processes (Fig. 10). The correlation between parietal process development and absolute size of the frill, however, is imperfect. The most extreme exception to this pattern is TMP 1989.126.0001, which, based on several factors represents a sub-adult specimen, and bears unfused parietal processes of similar shape to other subadult specimens (e.g., TMP 1989.098.0001 and TMP 2009.080.0001). Despite its apparent young age, the parietal of this specimen greatly exceeds many adult specimens (e.g., CMN 344, TMP 1988.036.0020, TMP 2005.012.0058) in most size metrics. This indicates a discontinuity between apparent developmental age and size that may further confuse the understanding of ceratopsid ontogeny. This is consistent with a similar discontinuity seen in extant taxa (e.g., Petermann et al. 2017), and is related to high developmental variation in dinosaurs (Griffin and Nesbitt 2016).

Although *Styracosaurus* parietal processes transform greatly in absolute size late in ontogeny (Fig. 10), their relative sizes appear fixed early in ontogeny. In nearly all skulls, whether adult or subadult (TMP 2009.080.0001 and TMP 1989.098.0001), P3 is the longest, most massive spike, followed by P4, P5, and P6 respectively (UALVP 55900 in an exception), although the processes are relatively much smaller in the subadults. This suggests that it is possible to recognize and diagnose subadult specimens of *Styracosaurus*; although identification of younger specimens is likely more problematic. Once again TMP 1989.126.0001 represents an exception to an otherwise consistent pattern. The parietal processes, rather than being heteromorphic with P3 dominating followed by P4 and P5, are all similar in size and morphology (Fig. 10).

The absence of reasonably complete juvenile *Styracosaurus* parietals and the highly species-specific morphology of the parietal ornamentation (specifically the loci) of *Centrosaurus* (i.e., char. 59–71, 74–77 of Frederickson and Tumarkin-Deratzian 2014) limit our ability to make detailed comparisons of parietal ontogeny between *Centrosaurus* and *Styracosaurus*, but some basic patterns may exist. The median undulations along the midline bar are thought to become more pronounced through ontogeny in *Centrosaurus* (Frederickson and Tumarkin-Deratzian 2014). In contrast, in TMP 2009.080.0001 these are more developed than in many larger *Styracosaurus*

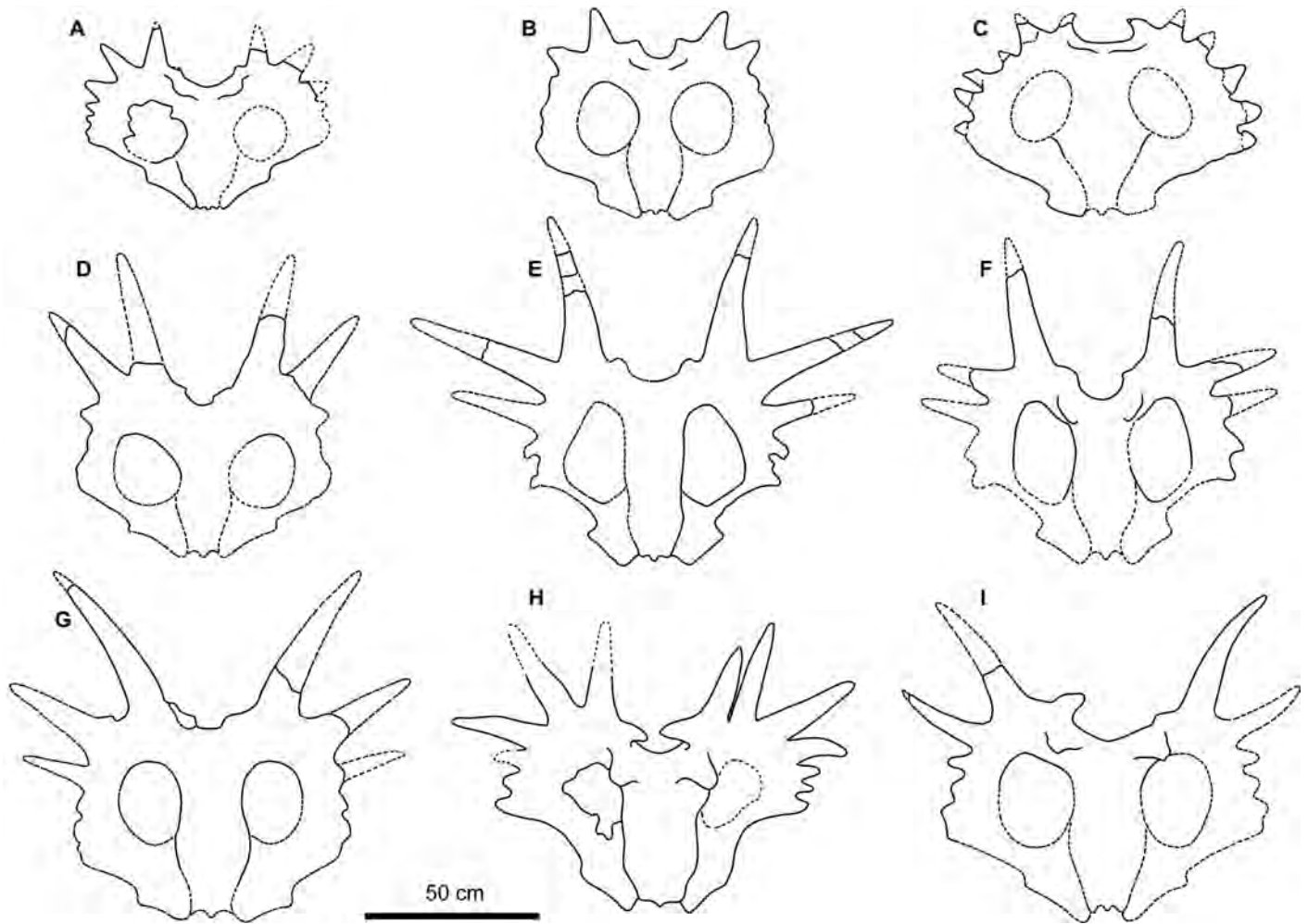


**Figure 10.** Reconstructed line drawings of the complete or relatively complete parietals of the centrosaurine ceratopsid *Styracosaurus albertensis* in dorsal (i.e., orthogonal to frill). Specimens are arranged in approximate order of increasing size of parietal ornamentation and size. A, TMP 2009.080.0001. B, TMP 1989.098.0001. C, TMP 1989.126.0001. D, TMP 1988.036.0020. E, CMN 344. F, TMP 2005.012.0058. G, TMP 1987.052.0001. H, UALVP 55900. I, ROM 1436. Based on development of the parietal ornamentation A–C represent subadult specimens, whereas D–I are regarded as largely skeletally mature. Scale bar = 50 cm.

specimens, suggesting an opposite trajectory or variability. Previous work has suggested that the frills of centrosaurines (Sampson et al. 1997), and specifically *Centrosaurus apertus* (Frederickson and Tumarkin-Deratzian 2014), become wider with age, with narrower morphologies restricted to smaller/younger forms. Sampson et al. (1997) argue that frill width in *Centrosaurus* is positively allometric, but the sample of very small *Centrosaurus* frills is limited. Although the smallest frill is distinctly narrow, most of the juvenile ontogenetic series is unknown, and all other specimens in their analysis traditionally identified as *Centrosaurus*, are adults or old adults (Sampson et al. 1997). None of these larger skulls show such a trend despite differing considerably in size. In the size series of *Styracosaurus* presented here, however, the smallest/youngest parietals are already broad, and retain broad aspect ratios in the largest

specimens, suggesting frill shape may be isometric. Two potential, but not mutually exclusive, conclusions can be drawn from these data. Firstly, it is possible that the frill of *Styracosaurus* is distinct from *Centrosaurus* in the allometry of the frill, specifically regarding the length/width ratio. If differences in frill allometry between these taxa exist, they may be reciprocal to the vast differences seen in parietal process allometry. Secondly, it is possible that much of this shape change is restricted to the earliest ontogenetic stages, and frills of ~80% maximum size or larger (the current *Styracosaurus* sample) are largely isometric with regard to frill shape. Additional young specimens are required to confirm frill allometry for both genera.

Taken together, the results suggest that there are subtle differences in the ontogeny of *Centrosaurus* and *Styracosaurus*, particularly with respect to nasal and postorbital horncores, and

parietals. It is worth noting that these differences in patterns of ontogenetic development (i.e., heterochrony) between these closely related taxa are largely restricted to the most diagnostic features, which have been hypothesized to be evolving under sociosexual selection (Sampson 1997, 1999; Padian and Horner 2011; Knell et al. 2013; Knapp et al. 2018).

### Qualifying Variation in *Styracosaurus* Parietal

**Processes:** Previous work on *Styracosaurus albertensis* has described significant variation within parietal ornamentation (Ryan et al. 2007; Holmes et al. 2020). This variation in parietal morphology is illustrated in Figures 2 and 10. While some of this variation, specifically the absolute sizes of the parietal processes (e.g., Fig. 10A–C), can be attributed to size and age of the individual (see previous section) not all of it can be explained in this way. Parietal processes 1 and 2 are quite variable in the extent of their expression, from indistinct or non-existent (e.g., CMN 344, TMP 1988.036.0020, 2016.012.0029) to moderate (TMP 1984.093.001, 2005.012.0058), to extensive, approaching *Centrosaurus* in size and shape (e.g., ROM 1436, UALVP 55900). Despite this variability, when present these processes are consistent in their positions and orientations. Process P1 originates from the anterodorsal surface of the posterior bar of the parietal posterior to the medial margin of the fenestra, and curves anterolaterally from this surface towards the fenestra. The only exception is an anomalous frill from BB 42 (TMP 1981.019.0249), which shows a very large P1 process in the normal position but projecting posterodorsally and curved posteriorly. Process P2 consistently originates on the posterior aspect of the posterior bar, just posterior to the base of P1, and projects posteromedially with a medial curvature. Processes P1 and P2 also appear to co-vary in their expression, such that when one is large, so is the other. Process P3 is (with the exception of UALVP 55900) consistently the largest parietal spike, in terms of both length and basal dimensions, and projects largely posteriorly, with a variable amount of curvature, generally laterally. Process P4 is similar to P3 but is generally slightly smaller (in length and basal diameter), projects posterolaterally, and appears to be more variable in both size and orientation than P3. Process P5 is variable in expression and can be a short tab (e.g., ROM 1436) or a true elongate spike (e.g., CMN 344, TMP 2005.012.0058, UALVP 55900). Processes 6, 7, and 8 (if present), are much smaller, and vary from modest scallops (e.g., ROM 1436, TMP 1987.052.001) to moderately sized tabs (e.g., CMN 344, TMP 2005.0012.0058, UALVP 55900).

Given the degree of variation with the parietal processes of *Styracosaurus*, it is worth considering the potential sources of this variation. *Styracosaurus* has been demonstrated to replace *Centrosaurus* within a constrained and well sampled formation. *Centrosaurus* is diagnosed based in part

on large P1 and P2 processes. Because these processes are highly variable in both size and shape in *Styracosaurus*, it is tempting to hypothesize an anagenic evolutionary trend from *Centrosaurus* to *Styracosaurus*, with a decrease in P1 and P2 expression through time. However, when the *Styracosaurus* specimens are placed in their stratigraphic positions within the formation (Fig. 2), no obvious correlation between P1 and P2 expression and stratigraphy is seen. Specimens with well-developed P1 and P2 processes can be found throughout the stratigraphic range of the species, both low (e.g., TMP 2005.012.0058) and high (e.g., UALVP 55900; Holmes et al. 2020). Similarly, specimens with indistinct or non-existent P1 and P2 processes can be found throughout the stratigraphic range of the species, both low (e.g., TMP 1987.052.0001) and high (e.g., TMP 1988.036.0020). Perhaps even more telling, extensive samples of parietals from *Styracosaurus* bonebeds (particularly BB42) show a high degree of variation within a single assemblage representing a herd, or at the very least a pencontemporaneous sample within the species. Frills from BB42 show a spectrum of P1 and P2 development from extensive (e.g., TMP1981.019.0249), to moderate (e.g., TMP 1966.010.0004, 1984.93.0001, 1999.055.0002, 1999.055.0005, 2001.012.0004) to indistinct processes (e.g., TMP 1981.019.0157). These results agree with Holmes et al. (2020) and are inconsistent with the idea that the variability in the frills of *Styracosaurus*, particularly the relative expression of P1 and P2, is due to a directional within-lineage (i.e., anagenesis) evolutionary trend from a *Centrosaurus*, or *Centrosaurus*-like, ancestor. This pattern is most consistent with a high level of variation in the parietal processes, particularly the development of P1 and P2, being maintained within the *Styracosaurus* population being sampled through fossils in the upper Dinosaur Park Formation. Given the current sample, the simplest explanation may be that the frill of *Styracosaurus* is just more variable in parietal morphology than closely related taxa, specifically *Centrosaurus*. This higher degree of variation may be due to stronger positive allometry acting on a greater number of parietal processes during growth.

It has been noted previously (Holmes et al. 2020) that parietal spike orientation appears to be correlated with the specific location that each spike occupies on the curved parietal margin, although this relationship was not quantified. In order to test this qualitative impression, we measured and plotted the position and orientation of each parietal spike—see Materials and Methods. The resulting plot (Fig. 11) confirms a close correlation between the position of the base of each epiparietal on the parietal margin and the orientation of its long axis with respect to the midline. Process 1 is the major exception to this pattern, but this may simply be because, unlike the other epiossifications, it

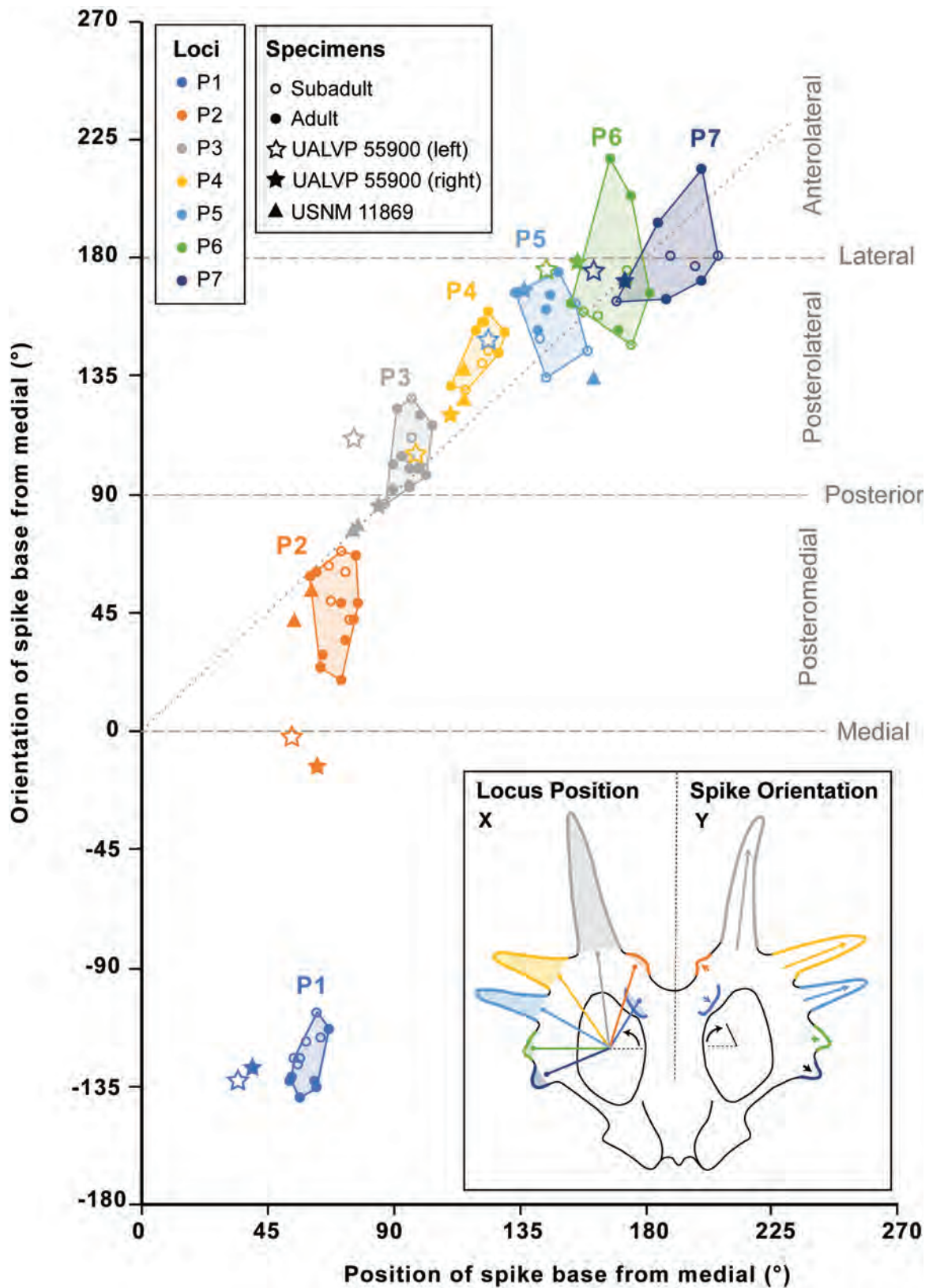


**Figure 11.** Graph depicting the orientation of each parietal process as a function of its radial position along the margin of the parietal. Serial homologous loci (i.e. P1–P7) are differentiated by colour and clusters are highlighted with convex hulls (excluding UALVP 55900, and USNM 11869). Horizontal dashed lines represent medial, posterior and lateral orientations. Diagonal dotted line represents 1:1 correlation in base opposition and process orientation. Immature specimens indicated with open circles, adult specimens indicated with solid circles, UALVP 55900 indicated with stars and USNM 11869 indicated by triangles.

originates from the dorsal surface of the parietal rather than from its periphery. The correlation with the remaining parietal loci is nearly 1:1 (a 1:1 relationship is illustrated by the diagonal dotted line in Fig. 11). Even further, homologous loci (e.g., P1, P2) generally plot consistently between specimens (UALVP 5590 is a conspicuous exception – see next paragraph) regardless of the perceived age of the specimen. In other words, the coloured convex hulls generally do not overlap and occupy unique areas. Of interest, parietal processes for subadult frills (i.e., TMP 1988.036.0020, TMP 1989.098.0001, TMP 1989.126.0001) do not show patterns distinct from those of the adult skulls, suggesting both the position of the epioassification loci and the orientation of the spine are conserved through ontogeny (at least through subadult and adult stages) and are therefore reliable taxonomic characters (Fig. 11).

The exception to this correlation between position and orientation is UALVP 55900, especially the left side, where a high degree of asymmetry with respect to the right side has accentuated the effect (Holmes et al. 2020). For P1 and P2, both left and right loci fall outside the area occupied by the other specimens. For P3, the left locus is an outlier and the right is slightly outside the hull. For P4, the left occurs centrally in the area occupied by P3 of other specimens, while the right falls between P3 and P4. A similar situation is seen for P5, where the left falls in the middle of the P4 data from the other specimens, and the right falls on the edge of the space occupied by the P5 of other specimens. This pattern continues for P6 and P7. Although the position of the left P3 does not overlap with the space occupied by any of the epioassifications of the other specimens, left P4 is similar to P3, left P5 is similar to P4, left P6 is similar to P5 and left P7 is similar to P6, while their right counterparts are relatively normal. It is possible that crowding produced by an extra epioassification on the left side (see Holmes et al. 2020) has caused the homologized loci to shift posteromedially along the curve of the parietal margin. Despite this odd asymmetry, the specimen nevertheless is diagnostic to *Styracosaurus albertensis*, and helps to emphasize the amount of variability and asymmetry that is possible within a clearly diagnosable taxon.

The enigmatic taxon *Styracosaurus* (= *Rubeosaurus*) *ovatus* (USNM 11869) from the upper Two Medicine Formation of Montana was also included in the plot. The positions and orientations of the P2 and P4 of this specimen do not deviate markedly from the other skulls, but the bases of both P3 loci are positioned farther medial, and their long axes are angled more strongly medially than any of the other skulls. It should be noted that there are now several other *Styracosaurus albertensis* specimens in which the P3 ossifications are less than 90° (i.e., oriented slightly medial), including TMP 2009.080.0001 and UALVP 55900.

However, USNM 11869 is the most extreme example of this medial projection. If the diagnosis of *S. ovatus* is based only on medially projecting P3 processes, then this also includes several specimens (i.e., TMP 2009.080.0001 and UALVP 55900) that are both morphologically consistent with *S. albertensis*, and derived from the restricted temporal and geographic range of *S. albertensis*. This supports the argument (Holmes et al. 2020) that *Styracosaurus ovatus* simply represents an extreme morph of *S. albertensis*, and is not a distinct taxon. At the very least, the diagnosis of *S. ovatus* is problematic and cannot rely solely on P3 processes that project posteromedially.

**Discussion of Epioassification Fusion:** In other small ceratopsid skulls (e.g., TMP 1989.126.0001, UALVP 40), the epioassifications are highly conspicuous, being little triangular structures attached, but not fused to, the apices of convexities distributed around the margin of the frill. As the skulls grew, the ossifications appear to have grown medially (both dorsally and ventrally) around the convexity, and eventually enveloped it so that the suture between the ossification and squamosal/parietal is located in line with the deepest point in the intervening scallops. Once they were fully coossified, the sutures became obscured. In the skulls where epioassifications are fully fused to the bone surface with the sutures not visible, or where the epioassification is absent, there is little option other than to measure the total distance from the deepest point of the scallop between epioassifications to the tip of the ossification/scallop. This may overestimate the total dimension of the ossification, because in some cases, the base of the ornament is actually formed by the underlying bone (i.e., squamosal or parietal). This appears to be the case in epiparietals 4, 5, and especially P6 of TMP 2009.080.0001. However, in some cases, textural differences between the bone surfaces of epioassifications and underlying bones might allow us to estimate the point of articulation. In TMP 2009.080.0001, P5 has a faint suture that coincides with the transition in texture (epioassification is rough, underlying bone smoother). In this case, the epioassification starts half way up the undulation. To a certain extent this distinction may be moot, as attempts to quantify the size and shape of the epioassification in isolation (i.e., excluding any contribution of the parietal/squamosal) and those investigating the entire process are asking very similar questions in the context of the evolution of these structures.

Although the edges of the squamosals of TMP 2009.080.0001 show the typical ‘scalloped’ pattern that indicates epioassification loci, there is no evidence of the ossifications themselves. Based on the size of the skull, one would have expected that they would be present, and at least partially fused. It is possible they had not fused to the squamosal at the time of death, and were disassociated

from the specimen prior to burial. In direct contrast, the epiparietals are not only present, but they are well coossified, to the degree that the sutures are hard to see. The only exception is one epiparietal (between the right P6 and P7) that shows a distinct suture. It is unclear why the states of development of the squamosal and parietal are so out of sync, but for this specimen it seems to be the case. How pervasive this heterochronic pattern is across *Styracosaurus* or Ceratopsidae, and its potential use in comparing developmental timing is unclear.

Sampson et al. (1997) and Frederickson and Tumarkin-Deratzian (2014) suggested that both epiparietals and episquamosals of *Centrosaurus* fuse to the frill in a posterior to anterior sequence. Whatever the case for the sequence of epiparietal fusion in centrosaurines, some *Centrosaurus* specimens (e.g., UALVP 11735) show the opposite pattern, with the fusion of episquamosals being most advanced anteriorly as in the case of *Chasmosaurus* (Godfrey and Holmes 1995). Unfortunately, no episquamosals are preserved in TMP 2009.080.0001, so it does not inform this question. In any case, this remains a potentially important question, as Frederickson and Tumarkin-Deratzian (2014) point out, epiossification fusion is a reliable ontogenetic indicator in *Centrosaurus*, and so potentially it may also be in the closely related *Styracosaurus*.

## CONCLUSIONS

The *Styracosaurus* specimen TMP 2009.080.0001, although about 80% of the size of the largest skull, exhibits many distinctly immature features, in particular small, triangular parietal epiossifications; a small, thin, recurved nasal horncore; and low, rounded postorbital horncores. This indicates that the pronounced cranial ornaments of adult individuals did not develop at a constant rate as the animal grew, but appeared rapidly only during the last stages of ontogeny. Nevertheless, subtle differences between these ossifications (e.g., P3 is measurably larger than any other epiparietal ossification, even in small individuals) should allow immature individuals of *Styracosaurus* to be identified.

Skull ontogeny of *Styracosaurus* resembles that of *Centrosaurus* and centrosaurines in general, but the timing of some events appears to be different, with some being accelerated (e.g., rate of growth as well as fusion of the nasal horncores, timing of cessation of growth of postorbital horncores), others delayed (e.g., development of parietal ornamentation, change in shape of nasal horncore, development of orbital horncores), or truncated (e.g., shape change in nasal horncores). In many cases, ontogenetic changes within one area of the skull (e.g., nasal) have become decoupled from general skull ontogeny, with each feature

following its own ontogenetic rate and trajectory. In one case, an intermediate growth stage is eliminated (e.g., loss of the tall, pointed, 'pyramidal' orbital horncores of subadult *Centrosaurus*), or in another case, reversed (e.g., sagittal bumps on the medial parietal bar of *Styracosaurus* reduced in size during growth, but became larger in *Centrosaurus*). Taken together, these suggest that many of the diagnostic differences between *Styracosaurus* and *Centrosaurus* are the result of heterochrony of the cranial ornaments.

Parietal ornamentation in *Styracosaurus* is more variable than in *Centrosaurus*. In some skulls, P1 can be expressed as a subtle bump on the posteromedial rim of the parietal, while in other skulls, it is prominent, in some cases forming a large anteriorly curving hook. Parietal process 2 is totally absent in a few skulls, but in others, it is expressed as a large, medially curving hook approaching the size and morphology exhibited by *Centrosaurus*. Process 3 is more consistent in morphology. Although small in small skulls, it exhibits strong positive allometry. It is nearly always the largest epiparietal. Process 4 is slightly smaller than P3, but is generally otherwise similar, although its morphology is more variable. Processes 5–7 also exhibit more variability in both size and morphology. Although sizes of epiparietals appear to correlate positively with skull size, there is no evidence of an evolutionary trend in size or morphology of parietal ornamentation in *Styracosaurus*.

Parietal epiossification orientation with respect to the midline is quite variable in *Styracosaurus*, and can be asymmetric in individual skulls. The specific orientations of these ossifications are directly correlated with the position they occupy on the curved margin of the parietal, and neither parameter should be taken in isolation. This relationship is also consistent through ontogeny.

## ACKNOWLEDGEMENTS

Specimen TMP 2009.080.0001 was found by James Wood in 2018 and collected by Darren Tanke, Mark Mitchell, Donald Henderson, and Tai Kubo in 2009. The 2014 and 2016 field crews excavated additional material from *Styracosaurus* bonebeds BB042, BB130, and BB301, and the 2018 field crew found and excavated TMP 2018.012.0023. The Eastern Irrigation District (EID) provided access to lands for TMP 2005.012.0058, 2009.080.0001, 2018.012.0023, and BB130, and Lee Fryberger and family provided access to lands for the Fryberger Bonebed (BB301). Dinosaur Provincial Park staff provided field logistical support.

TMP 2009.080.0001 was largely prepared by Ian Macdonald and Darren Tanke, with assistance from Dawna Macleod, Judy Graham, and Quintin Pretorius. Collections access and assistance was provided by Brandon Strilisky,

Rebecca Sanchez, Tom Courtenay, Heather Feeney, and Rhian Russell (RTMP), Howard Gibbins and Clive Coy (UALVP), Margaret Currie and Kieran Shepherd (CMN) and Kevin Seymour and David Evans (ROM), Christina Barron-Ortiz (RAM). Howard Gibbins also provided additional details on UALVP 55900. David Eberth provided field assistance and data in placing specimens into their stratigraphic context. Ben Borkovic, David Eberth, David Evans, Michael Ryan, and Darren Tanke, provided useful discussions on *Styracosaurus*. Andrew Farke and Catherine Forster provided reviews that significantly improved the manuscript, while Jordan Mallon handled the editorial process. Financial support for this project was provided by the Royal Tyrrell Museum of Palaeontology and the Royal Tyrrell Museum Cooperating Society.

## LITERATURE CITED

- Brown, C.M. 2013. Advances in quantitative methods in dinosaur palaeobiology: a case study in horned dinosaur evolution. PhD Dissertation, Department of Ecology and Evolutionary Biology, University of Toronto, Toronto. 443 pp.
- Brown, C.M., A.P. Russell, and M.J. Ryan. 2009. Pattern and transition of surficial bone texture of the centrosaurine frill and their ontogenetic and taxonomic implications. *Journal of Vertebrate Paleontology* 29:132–141.
- Currie, P.J., R.B. Holmes, M.J. Ryan, and C. Coy. 2016. A juvenile chasmosaurine ceratopsid (Dinosauria, Ornithischia) from the Dinosaur Park Formation, Alberta, Canada. *Journal of Vertebrate Paleontology* 36: e1048348.
- Dodson, P. 1989. *Avaceratops lammersi*: a new ceratopsid from the Judith River Formation of Montana. *Proceedings of the Academy of Natural Sciences of Philadelphia* 138:305–317.
- Dodson, P., and P.J. Currie. 1988. The smallest ceratopsid skull — Judith River Formation of Alberta. *Canadian Journal of Earth Science* 24:926–930.
- Evans, D.C. 2007. Ontogeny and evolution of lambeosaurine dinosaurs (Ornithischia: Hadrosauridae). PhD Dissertation, Department of Ecology and Evolutionary Biology, University of Toronto, Toronto, Canada. 497 pp.
- Evans, D.C. 2010. Cranial anatomy and systematics of *Hypacrosaurus altispinus*, and a comparative analysis of skull growth in lambeosaurine hadrosaurids (Dinosauria: Ornithischia). *Zoological Journal of the Linnean Society* 159:398–434.
- Farke, A.A. 2010. Evolution, homology, and function of the supracranial sinuses in ceratopsian dinosaurs. *Journal of Vertebrate Paleontology* 30:1486–1500.
- Farke, A.A., D.J. Chok, A. Herrero, B. Sciolieri, and S. Werning. 2013. Ontogeny in the tube-crested dinosaur *Parasaurolophus* (Hadrosauridae) and heterochrony in hadrosaurids. *PeerJ* 1: e182.
- Frederickson, J.A., and A.R. Tumarkin-Deratzian. 2014. Craniofacial ontogeny in *Centrosaurus apertus*. *PeerJ* 2: e252.
- Gilmore, C.W. 1917. *Brachyceratops*, a ceratopsian dinosaur from the Two Medicine Formation of Montana, with notes on associated fossil reptiles. United States Geological Survey Professional paper 103:1–45.
- Gilmore, C.W. 1922. The smallest known horned dinosaur, *Brachyceratops*. United States National Museum Proceedings 61:1–45.
- Gilmore, C.W. 1930. On dinosaurian reptiles from the Two Medicine Formation of Montana. United States National Museum, Proceedings 77:1–39.
- Goodwin, M.B., W.A. Clemens, J.R. Horner, and K. Padian. 2006. The smallest known *Triceratops* skull: New observations on ceratopsid cranial anatomy and ontogeny. *Journal of Vertebrate Paleontology* 26:103–112.
- Griffin, C.T., and S.J. Nesbitt. 2016. Anomalously high variation in postnatal development is ancestral for dinosaurs but lost in birds. *Proceedings of the National Academy of Sciences* 113:14757–14762.
- Holmes, R., and M. Ryan. 2013. The postcranial skeleton of *Styracosaurus albertensis*. *Kirtlandia* 58:5–37.
- Holmes, R.B., W.S.I. Persons, B.S. Rupal, A.J. Qureshi, and P.J. Currie. 2020. Morphological variation and asymmetrical development in the skull of *Styracosaurus albertensis*. *Cretaceous Research* 107:16 pp.. DOI 10.1016/j.cretres.2019.104308
- Knapp, A., R.J. Knell, A.A. Farke, M.A. Loewen, and D.W. Hone. 2018. Patterns of divergence in the morphology of ceratopsian dinosaurs: sympatry is not a driver of ornament evolution. *Proceedings of the Royal Society B: Biological Sciences* 285:20180312.
- Knell, R.J., D. Naish, J.L. Tomkins, and D.W.E. Hone. 2013. Sexual selection in prehistoric animals: detection and implications. *Trends in Ecology & Evolution* 28:38–47.
- Lambe, L.M. 1913. A new genus and species of Ceratopsia from the Belly River Formation of Alberta. *Ottawa Naturalist* 27:109–116.
- Mallon, J.C., M.J. Ryan, and J.A. Campbell. 2015. Skull ontogeny in *Arrhinoceratops brachyops* (Ornithischia: Ceratopsidae) and other horned dinosaurs. *Zoological Journal of the Linnean Society* 175:910–929.
- McDonald, A.T. 2011. A subadult specimen of *Rubeosaurus ovatus* (Dinosauria: Ceratopsidae), with observations on other ceratopsids from the Two Medicine Formation. *PLoS ONE* 6: e22710.
- Padian, K., and J.R. Horner. 2011. The evolution of ‘bizarre structures’ in dinosaurs: biomechanics, sexual selection, social selection or species recognition? *Journal of Zoology* 283:3–17.
- Penkalski, P., and P. Dodson. 1999. The morphology and systematics of *Avaceratops*, a primitive horned dinosaur from the Judith River Formation (late Campanian) of Montana, with the description of a second skull. *Journal of Vertebrate Paleontology* 19:692–711.
- Petermann, H., N.M. Koch, and J.A. Gauthier. 2017. Osteohistology and sequence of suture fusion reveal complex environmentally influenced growth in the teiid lizard

- ard *Aspidoscelis tigris*—Implications for fossil squamates. *Palaeogeography, Palaeoclimatology, Palaeoecology* 475:12–22.
- Ryan, M.J. 1992. The taphonomy of a *Centrosaurus* (Ornithischia: Ceratopsidae) bone bed (Campanian), Dinosaur Provincial Park, Alberta, Canada. Masters thesis, Department of Biological Sciences. University of Calgary, Calgary. 526 pp.
- Ryan, M.J. 2007. A new basal centrosaurine ceratopsid from the Oldman Formation, Southeastern Alberta. *Journal of Paleontology* 81:376–396.
- Ryan, M.J., D.C. Evans, and K.M. Shepherd. 2012. A new ceratopsid from the Foremost Formation (middle Campanian) of Alberta. *Canadian Journal of Earth Sciences* 49:1251–1262.
- Ryan, M.J., R. Holmes, and A.P. Russell. 2007. A revision of the late Campanian centrosaurine ceratopsid genus *Styracosaurus* from the Western Interior of North America. *Journal of Vertebrate Paleontology* 27:944–962.
- Sampson, S. 1993. Cranial Ornamentations in Ceratopsid Dinosaurs: Systematic, Behavioural, and Evolutionary Implications. PhD Dissertation, Department of Zoology, University of Toronto, Toronto. 299 pp.
- Sampson, S.D. 1995. Two new horned dinosaurs from the Upper Cretaceous Two Medicine Formation of Montana: With a phylogenetic analysis of the Centrosaurinae (Ornithischia: Ceratopsidae). *Journal of Vertebrate Paleontology* 15:743–760.
- Sampson, S.D. 1997. Bizarre structures and dinosaur evolution; pp. 39–45 in *Dinofest International Proceedings*. Academy of Natural Sciences and Arizona State University.
- Sampson, S.D. 1999. Sex and destiny: the role of mating signals in speciation and macroevolution. *Historical Biology* 13:173–197.
- Sampson, S.D., M.J. Ryan, and D.H. Tanke. 1997. Craniofacial ontogeny in centrosaurine dinosaurs (Ornithischia: Ceratopsidae): taxonomic and behavioral implications. *Zoological Journal of the Linnean Society* 121:293–337.
- Scannella, J.B., D.W. Fowler, M.B. Goodwin, and J.R. Horner. 2014. Evolutionary trends in *Triceratops* from the Hell Creek Formation, Montana. *Proceedings of the National Academy of Sciences* 111:10245–10250.
- Sternberg, C.M. 1927. Horned dinosaur group in the National Museum of Canada. *Canadian Field Naturalist* 41:67–73.
- Tokaryk, T.T. 1997. First evidence of juvenile ceratopsians (Reptilia: Ornithischia) from the Frenchman Formation (late Maastrichtian) of Saskatchewan. *Canadian Journal of Earth Sciences* 34:1401–1404.
- Tumarkin-Deratzian, A.B. 2010. Histological evaluation of ontogenetic bone surface texture changes in the frill of *Centrosaurus apertus*; pp. 251–263 in M.J. Ryan, B.J. Chinnery-Algeier, and D.A. Eberth (eds.), *New Perspectives on Horned Dinosaurs, the Royal Tyrrell Museum Ceratopsian Symposium*. Indiana University Press, Bloomington.

Appendix 1. List of known *Styracosaurus albertensis* material.

Specimen	Status	Completeness	Growth Stage	Formation	Location	Stratigraphy (m)	UTM E (m)	UTM N (m)
<b>Skulls/Skeletons</b>								
AMNH 5372	<i>S. albertensis</i>	Partial skull, partial skeleton	Adult	DPF <sup>1</sup>	DPP <sup>2</sup> , Quarry 250	?	460620 5	621496
/TMP 2006.019.0005	( <i>S. parksi</i> holotype)							
CMN 344	<i>S. albertensis</i> (holotype)	Complete skull, skeleton	Adult	DPF	DPP; Quarry 016	43.5 - 47.5	472167.854	5622232.802
ROM 1436	<i>S. albertensis</i>	Partial parietal	Adult	DPF	DPP; Quarry?	?	?	?
TMP 1986.126.0001	<i>S. albertensis</i>	Partial skull (missing snout)	Sub-adult	DPF	DPP; Quarry 179	42	477272.81	5629801.12
TMP 1987.052.0001	<i>S. albertensis</i>	Nearly complete skull	Adult	DPF	DPP; Quarry 183	32.5 - 40.5	459304	5622636
TMP 1988.036.0020	<i>S. albertensis</i>	Partial parietal	Adult	DPF	DPP	6 m below Bearpaw	477238	5629954
TMP 1989.097.0001	<i>S. albertensis</i>	Parietal, partial face, nearly complete skeleton	Sub-adult	DPF	Sage Creek	< 10 m below LCZ	545347	5451507
TMP 2003.012.0168	cf. <i>S. albertensis</i>	Partial face (no frill, nasal horn)	Adult	DPF	DPP	41 - 43.5	475367	5625614
TMP 2005.012.0058	<i>S. albertensis</i>	Partial skull (missing snout)	Adult	DPF	DPP; Quarry 248	37 - 41.75	460563.258	5619572.455
TMP 2009.080.0001	<i>S. albertensis</i>	Complete skull, partial skeleton	Sub-adult	DPF	DPP; Quarry 268	48 - 52.4	461295	5617724
TMP 2018.012.0023	cf. <i>S. albertensis</i>	Partial skull (missing frill)	Adult	DPF	DPP; Quarry?	?	470825	5617226
UALVP 52612	<i>S. albertensis</i>	Most of skull, partial skeleton	Adult	DPF	DPP; Quarry 256	?	473923	5625835
UALVP 55900	<i>S. albertensis</i>	Complete skull, skeleton	Adult	DPF	Matziwan Creek, Quarry 262	?	441261	5630148
<b>Bonebeds</b>								
<i>Styracosaurus</i> Bonebed - BB42	<i>S. albertensis</i>	267 Elements: 51 P, 48 FR, 21 SQ, 12 NA, 12 PO, 9 horn		DPF	DPP	29 - 30	465170	5620970
Princess Coulee Mouth BB - BB130	<i>S. albertensis</i>	2 parietal, 1 nasal		DPF	DPP	44.25 - 50.25	461460	5620680
Fryberger Bonebed - BB301/BB264	<i>S. albertensis</i>	144 Elements: 5 P, 14 FR, 5 horncore, 3 SQ		DPF	DPP	40 - 41.5	462702	5624733

<sup>1</sup>DPF = Dinosaur Park Formation<sup>2</sup>DPP = Dinosaur Provincial Park

Appendix 2. Radial position of base (position, °) and orientation from base to apex (projection, °) of each parietal spike for reasonably complete parietals of *Styracosaurus*, as plotted in Figure 11. The circular coordinate takes origin at the centre of the fenestra, with 0° orientated medial, 90° oriented posterior, and 180° oriented lateral. See inset of Figure 11 for diagram.

Parietal Horn ID	TMP 1989.097.0001		TMP 1986.126.0001		ROM 1436		CMN 344		TMP 2005.012.0058	
	Postion	Projection	Postion	Projection	Postion	Projection	Postion	Projection	Postion	Projection
P1 R	59	241	57	235	67	246	—	—	62	226
P1 L	64	243	63	252	63	224	—	—	54	228
P2 R	67	62	72	68	73	34	—	—	72	48
P2 L	73	60	75	42	76	42	77	66	65	28
P3 R	96	103	97	126	104	116	100	100	96	99
P3 L	97	111	99	—	100	120	99	99	90	91
P4 R	124	144	125	—	130	151	123	155	124	159
P4 L	122	139	124	—	—	—	122	155	120	152
P5 R	145	134	155	162	149	174	—	—	—	—
P5 L	143	149	160	144	—	—	146	165	145	160
P6 R	174	175	175	146	171	152	—	—	—	—
P6 L	163	157	174	170	—	—	168	217	175	203
P7 R	189	180	198	176	188	164	—	—	—	—
P7 L	NA	NA	206	180	—	—	185	193	200	213

Parietal Horn ID	TMP 1987.051.0001		TMP 1988.036.0020		TMP 1999.055.0005		TMP 1984.043.0001		TMP 2009.080.0001	
	Postion	Projection								
P1 R					245		57	220	55	235
P1 L					241		53	226	56	233
P2 R	63	60	64	24	72	19	68		68	49
P2 L			61	58	78	48			69	
P3 R	92	122	88		96	93	96	92	87	86
P3 L	93	104	90	101	102	97			87	
P4 R			111	131					116	129
P4 L	128	143	114						114	
P5 R			134	166					142	152
P5 L	157									141
P6 R			154	162					158	159
P6 L	182	166							157	
P7 R									170	163
P7 L	200	171								

Parietal Horn ID	USNM 11869		UALVP 55900	
	Postion	Projection	Postion	Projection
P1 R			40	231
P1 L			35	226
P2 R	61	53	63	346
P2 L	55	41	54	357
P3 R	78	77	85	85
P3 L	76	75	76	110
P4 R	115	137	111	120
P4 L	115	125	98	105
P5 R			137	167
P5 L	162	133	124	148
P6 R			156	178
P6 L			145	175
P7 R			173	171
P7 L			162	174
P8 R				
P8 L			175	188

## Appendix 3. Specimen numbers for nasal and postorbital horncores included in Figures 7 and 8.

<b>Nasals</b>									
#	Specimen #	Basal Size	Fusion	Reflected	#	Specimen #	Basal Size	Fusion	Reflected
1	TMP1995.400.0074	72	unfused	yes	54	TMP1998.093.0163	77	unfused	no
2	TMP1996.012.0286	81	unfused	no	55	TMP2009.031.0001	190	fused, isolated	yes
3	TMP1996.012.0288	82	unfused	no	56	TMP2009.080.0001	191	fused, articulated	no
4	TMP2009.400.0004	104	unfused	yes	57	TMP1966.010.0023	194	fused, Isolated	no
5	TMP1995.400.0265	117	unfused	yes	58	TMP1966.010.0019	212	fused, Isolated	yes
6	TMP1992.036.0442	134	unfused	no	59	TMP1966.010.0021	213	fused, Isolated	yes
7	TMP1981.026.0003	139	unfused	yes	60	TMP2017.023.0016	223	fused, associated	
8	TMP2014.017.0064	147	unfused	yes	61	TMP2005.012.0058	225	fused, articulated	yes
9	TMP1982.018.0220	166	unfused	no	62	TMP1966.010.0020	226	fused, Isolated	yes
10	TMP1993.036.0435	167	unfused	yes	63	TMP1966.010.0022	250	fused, Isolated	yes
11	TMP2009.039.0365	168	unfused	no	64	UAVLP 55900	257	fused, articulated	no
12	TMP1995.400.0187	140	tip fused	yes	65	TMP2018.012.0023	259	fused, associated	no
13	TMP1995.401.0084	143	tip fused	no	66	UALVP 52612	264	fused, articulated	yes
14	TMP2016.016.0002	158	tip fused	yes	67	CMN 344	283	fused, articulated	no
15	TMP1966.033.0017	165	tip fused	yes	68	TMP1987.052.0001	321	fused, articulated	yes
16	TMP1979.011.0083	167	tip fused	yes					
17	TMP1997.145.0074	172	tip fused	no					
18	TMP1980.024.0004	173	tip fused	no					
19	TMP2016.016.0029	176	tip fused	no					
20	TMP1995.175.0019	179	tip fused	no					
21	TMP1981.022.0010	185	tip fused	no					
22	TMP1980.018.0310	192	tip fused	no					
23	TMP1982.018.0044	198	fused, Isolated	no					
24	TMP1987.018.0039	207	fused, Isolated	no					
25	TMP1965.023.0019	220	fused, Isolated	no					
26	TMP1981.018.0183	222	fused, Isolated	no					
27	TMP1982.018.0281	222	fused, Isolated	yes					
28	TMP1995.401.0045	223	fused, Isolated	no					
29	TMP1987.018.0020	224	fused, Isolated	yes					
30	TMP1993.036.0587	226	fused, Isolated	no					
31	TMP1982.018.0067	230	fused, Isolated	yes					
32	TMP1991.018.0090	246	fused, Isolated	no					
33	TMP1992.036.0712	247	fused, Isolated	yes					
34	RAM P 64.5.191	248	fused, Isolated	no					
35	TMP1994.012.0525	255	fused, Isolated	no					
36	TMP 1992.082.0001	192	fused, articulated	yes					
37	ROM 767	195	fused, articulated	no					
38	CMN 8798	201	fused, articulated	yes					
39	CMN 437 (LAVAL)	206	fused, articulated	yes					
40	YPM 2015	206	fused, articulated	yes					
41	TMP1980.024.0004	211	fused, articulated	yes					
42	TMP1993.036.0117	235	fused, articulated	no					
43	CMN 8795	235	fused, articulated	yes					
44	TMP1994.182.0001	241	fused, articulated	no					
45	TMP2006.025.0001	252	fused, articulated						
46	TMP2015.018.0014	258	fused, articulated	yes					
47	AMNH 5351	259	fused, articulated	no					
48	UALVP 11735	202	fused, articulated	no					
49	CMN 11837	214	fused, articulated	yes					
50	CMN 348	232	fused, articulated	yes					
51	ROM 43214	242	fused, articulated	yes					
52	AMNH 5239	264	fused, articulated	no					
53	TMP1997.085.0001	267	fused, articulated	yes					
<b>Postorbitals</b>									
#	Specimen #	Basal Size	Side	Fusion	Res. Pit	Refl'd			
1	TMP1980.016.1694	22	right	unfused	no	no			
2	TMP1979.011.0157	38	left	unfused	no	yes			
3	TMP1980.018.0016	39	right	unfused	no	no			
4	TMP1982.018.0139	47	left	unfused	no	yes			
5	TMP1995.400.0164	52	left	unfused	no	yes			
6	TMP1995.400.0114	53	left	unfused	no	yes			
7	TMP1979.011.0117	74	right	unfused	no	no			
8	TMP1981.022.0013	74	right	unfused	no	no			
9	TMP1995.400.0256	78	right	unfused	no	no			
10	TMP1992.036.0398	78	right	unfused	no	no			
11	TMP1980.016.1043	80	right	unfused	no	no			
12	TMP1995.401.0107	80	right	unfused	no	no			
13	TMP1979.011.0020	82	left	unfused	no	yes			
14	TMP1979.011.0100	85	left	unfused	no	yes			
15	TMP1989.018.0064	88	right	unfused	no	no			
16	TMP2008.079.0047	88	right	unfused	no	no			
17	TMP2013.044.0027	89	right	unfused	no	no			
18	TMP1994.012.0942	90	right	unfused	no	no			
19	TMP1986.018.0058	93	left	isolated	no	yes			
20	TMP1997.012.0192	93	right	unfused	no	no			
21	TMP1992.036.1017	98	left	unfused	no	yes			
22	TMP1982.018.0017	105	left	unfused	no	yes			
23	TMP2015.059.0023	105	left	partial	no	yes			
24	TMP1998.093.0034	109	left	fused	no	yes			
25	TMP2005.009.0007	111	left	unfused	no	yes			
26	TMP1994.012.0154	111	left	unfused	no	yes			
27	TMP1979.011.0163	125	right	fused	no	no			
28	TMP1994.012.0524	130	right	unfused	no	no			
29	TMP1997.012.0213	135	left	fused	no	yes			
30	ROM 767	144	both	fused	no	no			
31	TMP1982.018.0104	145	left	fused	no	yes			
32	TMP1988.036.0269	150	right	fused	no	no			
33	TMP2014.017.0054	150	left	fused	no	yes			

## Appendix 3 continued

Postorbitals							#	Specimen #	Basal Size	Side	Fusion	Res.	Pit	Refl'd	
#	Specimen #	Basal Size	Side	Fusion	Res.	Pit	Refl'd	#	Specimen #	Basal Size	Side	Fusion	Res.	Pit	Refl'd
34	CMN 8797	166	both	fused	no	yes	yes	75	TMP1980.018.0083	136	left	fused	yes	yes	
35	CMN 348	169	both	fused	yes	yes	yes	76	TMP1989.018.0040	137	left	fused	yes	yes	
36	UALVP 11735	177	both	fused	no	no	no	77	TMP1979.011.0041	139	left	fused	yes	yes	
37	TMP1982.018.0262	93	left	unfused	no	yes	yes	78	TMP2014.017.0011	139	left	fused	yes	yes	
38	TMP1979.011.0066	94	right	unfused	no	no	no	79	TMP1979.011.0085	141	left	fused	yes	yes	
39	TMP2014.017.0024	101	right	uncertain	no	no	no	80	TMP1980.016.0515	147	left	fused	yes	yes	
40	TMP1980.018.0315	107	left	unfused	no	yes	yes	81	TMP1979.011.0040	155	right	fused	yes	no	
41	TMP2014.017.0008	115	right	fused	no	no	no	82	TMP1995.012.0145	157	right	fused	yes	no	
42	TMP1979.011.0031	116	left	unfused	no	yes	yes	83	TMP1980.018.0303	158	right	fused	yes	no	
43	TMP1980.018.0295	117	left	fused	no	yes	yes	84	YPM 2015	160	both	fused	yes	yes	
44	TMP2014.017.0030	121	left	partial	no	yes	yes	85	TMP1994.182.0001	164	both	fused	yes	no	
45	TMP1994.012.0940	127	left	partial	no	yes	yes	86	TMP1993.070.0001	167	both	fused	yes	yes	
46	TMP1979.011.0120	137	right	fused	no	no	no	87	CMN 8795	173	both	fused	yes	yes	
47	TMP1982.018.0002	138	left	fused	no	yes	yes	88	TMP1982.019.0244	106	right	fused	yes	no	
48	TMP2016.016.0031	144	right	fused	no	no	no	89	TMP1979.010.0005	108	both	fused	yes	no	
49	TMP1995.401.0044	154	left	fused	no	yes	yes	90	TMP1979.011.0080	116	right	fused	yes	no	
50	TMP1994.012.0158	93	left	fused	yes	yes	yes	91	TMP 1965.012.0005	130	right	fused	yes	no	
51	TMP1980.016.1677	101	right	unfused	no	no	no	92	NHM R 4859	131	both	fused	yes	yes	
52	TMP1980.018.0309	105	left	fused	no	yes	yes	93	TMP1965.023.0027	134	right	fused	yes	no	
53	TMP1988.036.0033	107	right	unfused	no	no	no	94	TMP2015.024.0069	137	left	fused	yes	yes	
54	TMP1989.018.0009	109	left	fused	no	yes	yes	95	AMNH 5351	151	both	fused	yes	no	
55	TMP1980.018.0221	119	right	partial	no	no	no	96	USNM 12742	160	left	fused	yes	yes	
56	TMP1979.011.0084	122	left	fused	no	yes	yes	97	CMN 347	169	both	fused	yes	no	
57	CMN 8798	124	both	fused	no	yes	yes	98	TMP1997.085.0001	185	both	fused	yes	yes	
58	TMP1980.018.0350	127	left	fused	no	yes	yes	99	TMP2014.015.0084	63	left	unfused	no	yes	
59	TMP1992.036.0650	128	left	fused	no	yes	yes	100	TMP2009.031.0012	95	right	unfused	no	no	
60	TMP1979.011.0128	135	left	fused	no	yes	yes	101	TMP1998.093.0064	95	right	partial	no	no	
61	TMP1979.011.0129	136	left	fused	no	yes	yes	102	TMP2009.080.0001	109	both	partial	no	no	
62	TMP1994.012.0838	138	right	fused	no	no	no	103	TMP2018.012.0013	109	left	fused	no	yes	
63	TMP1982.016.0178	145	right	fused	no	no	no	104	TMP1986.126.0001	109	both	fused	no	yes	
64	TMP1979.011.0081	145	right	fused	no	no	no	105	TMP1966.010.0041	109	left	fused	no	yes	
65	TMP1995.401.0004	146	right	fused	uncertain	no	no	106	TMP2014.015.0143	120	left	partial	no	yes	
66	TMP1989.018.0024	149	left	fused	no	yes	yes	107	TMP2007.012.0059	123	left	fused	no	yes	
67	TMP1979.011.0089	154	right	fused	no	no	no	108	TMP2003.012.0168	124	left	fused	no	yes	
68	AMNH 5429	162	both	fused	no	no	no	109	TMP1990.058.0004	120	right	fused	yes	no	
69	AMNH 5239	167	both	fused	no	yes	yes	110	CMN344	123	both	fused	yes	yes	
70	TMP1986.018.0050	116	left	fused	yes	yes	yes	111	TMP2002.070.0001	124	left	fused	yes	yes	
71	TMP1967.020.0234	117	right	fused	yes	no	no	112	UALVP 52612	125	both	fused	yes	yes	
72	TMP1992.082.0001	119	left	fused	yes	yes	yes	113	TMP2005.012.0058	126	right	fused	yes	no	
73	TMP1986.018.0101	120	left	fused	yes	yes	yes	114	UALVP 55900	140	both	fused	yes	no	
74	TMP1983.018.0037	135	left	fused	yes	yes	yes	115	TMP2014.015.0094	149	right	fused	yes	no	